A KINETIC AND SPECTROSCOPIC INVESTIGATION OF THE CHEMISTRY OF 4-AZIDOPYRIDINE-1-OXIDE

An Honors Thesis (HONRS 499)

by

Kyle Crabtree

Thesis Advisor: James S. Poole

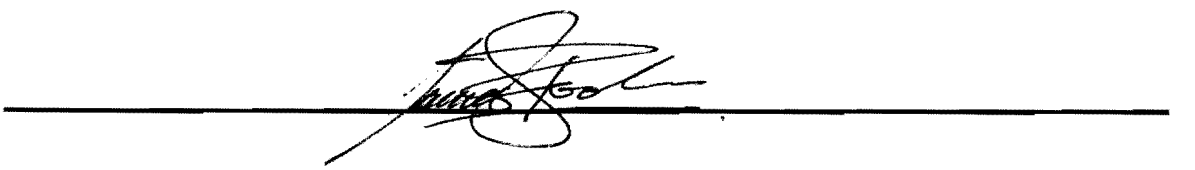

Ball State University

Muncie, Indiana

December 2006

Expected Date of Graduation: December 2006

Table of Contents

Table of Figures

Table of Schemes

Table of Tables

Acknowledgements

First, I would like to thank my advisor, Dr. Poole. Not only was he immensely helpful in all aspects of this project for the last year and a half, but he has also given me a number of opportunities I never imagined having upon entering college. Because of him, I have been able to have the privilege of presenting this research at a number of scientific venues, but more importantly, his guidance has given me a great deal of confidence in myself for my future career in graduate school and beyond. I consider myself very fortunate to have been a member of his group during my time here.

I would also like to thank my lab partner, Chad Gibson. When experiments were failing, or the labwork reached a tedious stage, he was always able to get me refocused. Whether it was by playing a hand of cards, having a pointless debate over silly, meaningless topics like whether or not his coat should be considered a motorcycle jacket (no doubt the other people working in CP 442 would attest to the intensity with which we debated, and moreover the inanity of the topics), or talking about football, he always found a way to keep us both entertained, which, in a lab environment is often necessary to regain focus.

Finally, I owe much, if not all of the credit for this work to my wife, Debra. When our son was born, it would have been very easy for me to abandon my research in favor of being at home. However, she made a great number of sacrifices and displayed an incredible amount of patience that enabled me to accomplish much more than would have otherwise been possible. For all that, I am indebted to her.

Summary

STUDENT: Kyle Crabtree

ADVISOR: James S. Poole

TITLE: A Kinetic and Spectroscopic Investigation of the Chemistry of 4-Azidopyridine-1-Oxide

In this project, we studied two different chemical reactions that the title compound can undergo. The first was a photochemical process, meaning that the molecule absorbs light and then undergoes a transformation. Simpler versions of the type of compound we chose have been studied in the past, and we discovered that this compound's photochemical reactivity was rather different from those simpler versions. We then studied the reaction under different conditions and, using a variety of analytical techniques as well as, have hypothesized what the products of these other reactions are.

Another reaction we studied is what is known as a 1,3-dipolar cycloaddition reaction. It was known from previous studies that 4-azidopyridine-1-oxide exhibits different cycloaddition chemistry than other compounds. By performing a systematic series of experiments, we have derived important information about the rate of the reaction, and that information has allowed us to draw conclusions about how the reaction itself occurs on a physical level.

Abstract

STUDENT: Kyle Crabtree

ADVISOR: James S. Poole

TITLE: A Kinetic and Spectroscopic Investigation of the Chemistry of 4-Azidopyridine-1-Oxide

The photochemistry of 4-azidopyridine-1-oxide was investigated by room-temperature laser flash photolysis, glass matrix photolysis with ultraviolet/visible spectroscopy and product analysis nuclear magnetic resonance spectroscopy, and electron paramagnetic resonance spectroscopy. It was determined that at room temperature, intersystem crossing to the triplet state is the dominant process, yielding 4,4'-axobis(pyridine-1-oxide) as the only photoproduct.

After photolysis in a 3-methylpentane glass matrix at 77K, strong NMR and HPLC evidence suggested that hydrogen abstraction from the solvent is the dominant process, yielding 4-(1'-ethyl-1'-methylpropyl)aminopyridine-1-oxide. This result was consistent with the results of a comparative study of the same process with the isomeric 3-azidopyridine-1-oxide. Photolysis in 2-methyltetrahydrofuran glass gave a complicated product mixture that was not investigated further.

A kinetic investigation of the 1,3-dipolar cycloaddition reaction of 4-azidopyridine-1-oxide with methyl acrylate in acetonitrile yielded a second-order overall rate coefficient of 1.00×10^{-5} $M^{-1}s^{-1}$ at 323 K. From this study, it was also concluded that the first cycloaddition step in the mechanism of the reaction is rate-determining.

Chapter 1- Literature Background

1.1- Introduction

Aryl azides have been investigated with great interest during the previous century not only due to their many applications in industry and biological chemistry, but also because of the basic mechanistic questions they have raised. Researchers have been intrigued by the variety of products these compounds afford under various conditions, and many proposals have been made concerning the exact nature of the intermediates involved in these reactions.

An important industrial use for aryl azides can be found in the area of photolithography, in which they function as photoresists.[1] Furthermore, they are involved in the development of contrast-enhancing layers used especially in the manufacture of increasingly small circuit microchips.[2] A related application of the photolysis of aryl azides is the manufacture of electrically-conducting polymers, which can be generated by the oxidation of the primary polymeric photoproducts of these compounds.[3]

Aryl azides have also attracted attention from researchers in the field of biological chemistry. Phenyl azide and its derivatives have been utilized in the process of photoaffinity labeling.[4] The basic principle of photoaffinity labeling is that a molecule bearing a photolabile group is introduced into a macromolecule of interest, where it is photolyzed. Ideally, a highly reactive intermediate is formed, which rapidly bonds covalently with a biologically important area of the macromolecule, yielding a characterizable product.[5]

Finally, aryl azides are important in organic synthesis.[6] They are one of the most important routes to generating 1-aryl-4-substituted-[1,2,3]-triazoles, which are synthesized by reaction of the aryl azide with a terminal alkyne using a Cu(I) catalyst.[7] The regioselectivity of these types of reactions can also be reversed; indeed, aryl azides have also been used in the synthesis of 1-aryl-5-amido-[1,2,3]-triazolines by the reaction of aryl azides with enamides in the absence of a catalyst.[8]

1.2- The Chemistry of Phenylnitrene

1.2.1- Phenylnitrene vs. Phenylcarbene

The simplest aryl azide that can be considered is phenyl azide. This compound can decompose thermochemically or photochemically to generate phenylnitrene (PhN).[9,10] In order to understand the reactivity of PhN, it is important to consider this species' electronic structure and how it differs from the isoelectronic phenylcarbene (PhCH).

According to Borden *et. al.*[11], nitrenes and carbenes are similar in the fact that each is a neutrally-charged species that contains two valence electrons distributed between two non-bonding molecular orbitals. In PhCH, these two orbitals are a pure 2p-π atomic orbital and a normal σ molecular orbital. Due to its greater s-character, the latter is selectively stabilized, resulting in a closed-shell singlet ($^1A_1$) as the lowest-energy singlet state. Nevertheless, due to Coulombic repulsion, the triplet ($^3A_2$) state, in which the two non-bonding molecular orbitals are singly occupied with electrons of opposite

spins, is the ground state of PhCH. The energy between the ground triplet state and the lowest singlet state (ΔE_{ST}) is 2.3 kcal/mol.[12]

The ground state of PhN, like PhCH, is the triplet state.[11] However, the two non-bonding molecular orbitals between which these two electrons are distributed are both pure 2p atomic orbitals, which should be degenerate. Therefore, to a first approximation, the lowest-energy singlet state should be the $^1A_1$ state, since the phenyl substituent should lift the degeneracy of the 2p orbital coplanar with the π orbitals in the ring. However, calculations[13] show that instead, the open-shell singlet ($^1A_2$) is selectively stabilized.

Figure 1- Electronic Structure of Phenylnitrene

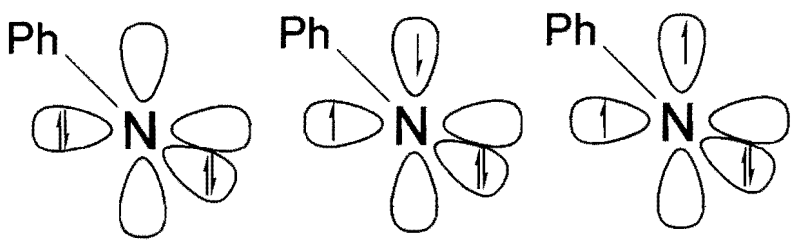

$^1A_1$ $^1A_2$ $^3A_3$

The reason for this is that the electron in the coplanar 2p orbital is almost completely delocalized within the aromatic ring, resulting in what resembles an iminyl-cyclohexadienyl biradical. This delocalization reduces the Coulombic repulsion present in the $^1A_1$ state,[14] thereby lowering the relative energy of the $^1A_2$ state. Due to these inherent differences in electronic structure, ΔE_{ST} for PhN is larger than PhCH. These two factors help explain the unique reactivity of PhN, especially as compared to PhCH.

1.2.2- Electronic State Energies of Phenylnitrene

As mentioned above, the unique electronic structure of PhN accounts for its reactivity. To determine the energies of the $^1A_2$ and $^1A_1$ states relative to the $^3A_2$ ground state, electron detachment spectroscopy was employed.[15,16] This experiment involves reaction of phenyl azide with an electron, which generates molecular nitrogen and the phenylnitrene anion. A spectrum of this species is collected, and from the photodetachment onset wavelengths, the energy levels for phenylnitrene can be determined. Early studies found ΔE_{ST} = 4.3 kcal/mol,[15] but later, more refined studies gave a value of 18.3±0.2 kcal/mol,[16] in excellent agreement with high-level calculations.[17]

1.2.3- Reactions of Phenylnitrene

In most studies of reactive intermediates, information is gained by studying the product mixtures obtained from reactions with a number of trapping reagents. However, it was found that the main product of azide photolysis and thermolysis was a polymeric tar.[3,18] As a result, empirical research on PhN was somewhat retarded compared to research on PhCH. Nevertheless, although PhN could not be directly trapped, it was observed that solution-phase thermolysis of phenyl azide in the presence of aniline gives azepine **5** (Scheme 1).[19] The trappable intermediate was proposed to be either benzazirene **3** or 1,2-didehydroazepine **4**, either of which formed by rearrangement of singlet PhN (^{1}**2**). It was later shown that photolysis of phenyl azide in the presence of diethylamine yielded a similar product.[20]

Under different conditions, however, chemical analysis of the product mixtures was found to give supporting evidence for other pathways. At low concentrations of phenyl azide, polymer was not formed; instead, azobenzene (**6**, below) was the dominant product,[21] although it is still unclear whether this is due to ^{3}**2** dimerization or its reaction with **1**. Gas-phase pyrolysis of **1** was found to lead to the formation of the cyanocyclopentadienyl radical[22] (Scheme 2), while photolysis at 77K in organic glasses again gave **6** after the reaction mixture was allowed to warm to room temperature.[23] Low-temperature matrix isolation IR spectroscopy detected **4**,[24] and it was confirmed that **4** was the species trapped by nucleophiles in solution to form **5**.[25]

Scheme 1- Solution Phase Thermolysis and Photolysis of Phenyl Azide

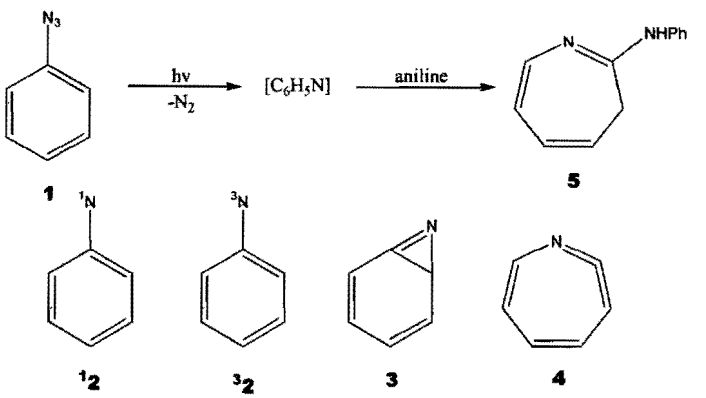

Scheme 2- Gas-phase Pyrolysis of Phenylnitrene

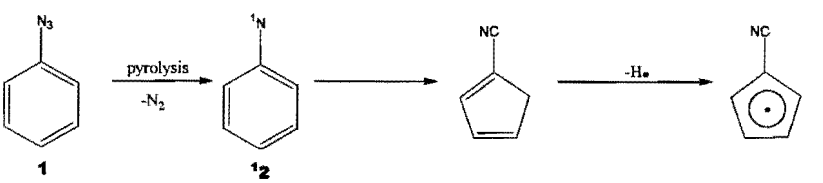

Scheme 3 illustrates the modern understanding of the chemistry of phenylnitrene. Upon decomposition of **1**, ^{1}**2** is formed and molecular nitrogen is released. In the gas phase, this species undergoes a vibrational rearrangement over an energy barrier of 30 kcal/mol to eventually give the cyanocyclopentadienyl radical,[26] which may react further. At room temperature, ^{1}**2** rearranges over a smaller energy barrier to **3**,[17,27] which then rearranges to **4**[24,25] and can be trapped. At low temperatures, intersystem crossing to ^{3}**2** becomes dominant. This species can then either dimerize or react with **1** to give **6**.[23] However, ^{3}**2** is photosensitive, and can react with light to give **4**,[23] which is responsible for the detection of this species in low-temperature matrices.[24]

Scheme 3- Reactions of Phenylnitrene

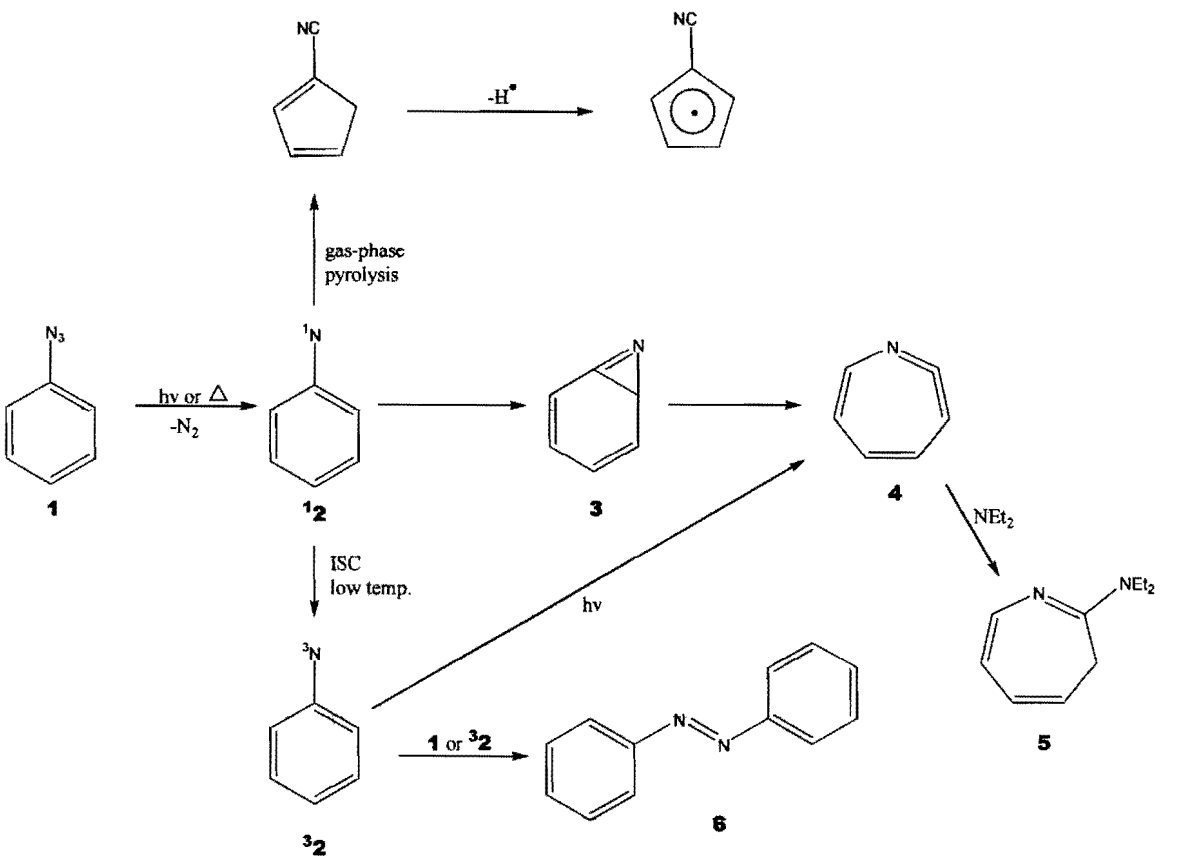

1.2.4- Substituent Effects: Intersystem Crossing and Cyclization of Phenylnitrene

In 1997, the direct observation of ^{1}**2** by UV/Visible spectroscopy was reported,[28,29] which allowed calculation of the barriers to rearrangement and intersystem crossing, along with the corresponding rate coefficients. This was performed by monitoring the first-order decomposition of ^{1}**2** to determine the observed rate coefficient (k_{OBS}) across a large temperature range. When the data were analyzed, it was discovered that a break point existed at around 165K where k_{OBS} became temperature-independent. It was confirmed[30] that this area corresponded to the rate coefficient of intersystem crossing (k_{ISC}), and that at any point, $k_{OBS} = k_{ISC} + k_R$ (the rate coefficient for rearrangement). These results are consistent with the observation that at low temperatures, intersystem crossing becomes the dominant process. In pentane, the value for k_{ISC} was found to be $(3.2 \pm 0.3) \times 10^6$ s^{-1}, and the barrier to cyclization to be 5.6 ± 0.3 kcal/mol.[31]

The rate of intersystem crossing of PhN can be affected by substituents on the phenyl ring. Substitution of both electron-donating and withdrawing groups at the *para* position on the ring increases the rate of intersystem crossing.[31-34] The two most significant factors responsible for the larger increases[35] are heavy-atom effects, such as those from Br and I,[32] and π-donating effects, such as those from a methoxy substituent.[32] *Ortho* substituents[22,30,33,34,36,37] behave slightly differently. Dialkyl substitution increases k_{ISC} more than monoalkyl substitution[30,36] due to electron-donating effects, while mono- and difluoro substitution have no significant effect.[37] Further studies are needed to understand exactly why these substituents affect intersystem crossing as they do.

Unlike with intersystem crossing, *para* substitution has no significant effect on and rearrangement and ring expansion of PhN. This should not be surprising, for as was shown before, ^{1}**2** exists in the $^1A_2$ state, and the first step in ring expansion is cyclization to **3**.[17,27] Therefore, only an out-of-plane bend of nitrogen is required for cyclization.[27] Only *p*-phenyl and *p*-cyano substituents significantly affect cyclization, slowing it slightly due to their ability to withdraw spin density from the *o*-carbon atom.[35] However, *ortho* substitution does affect the barrier to cyclization, as well as the regioselectivity of the rearrangement. Singly *o*-substituted phenylnitrenes cyclize away from the substituent; the barrier to cyclize toward the substituent is about 2.0 kcal/mol higher if the substituent is methyl.[36,38] Dimethyl substitution does raise the barrier to cyclization by 2.0 kcal/mol, as cyclization away from the substituent is impossible.[36,38] However, larger alkyl groups lower the increase in the barrier, even to the point that di-*tert*-butyl substitution actually has a lower barrier to cyclization than ^{1}**2**.[30]

A special case in cyclization and ring expansion chemistry of PhN is its pentafluoro- derivative. Unlike other singlet aryl nitrenes, this derivative has a long enough lifetime that it can be trapped with pyridine to form an ylide.[28] Due to its long lifetime, this singlet nitrene species is the one most useful for many of the applications discussed earlier.[35] Finally, another special case is *o*-phenyl substitution, as cyclization of this species leads to the formation of carbazoles upon pyrolysis[39] and photolysis.[40]

Scheme 4- Special Reactions of Phenylnitrene Derivatives

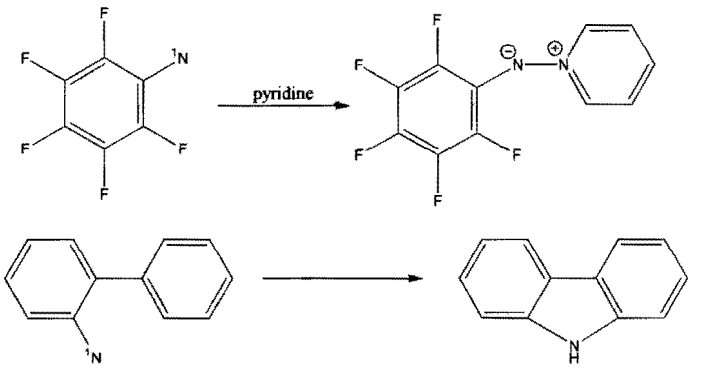

1.3- 1,3-Dipolar Cycloaddition Reactions of Aryl Azides

As mentioned earlier, aryl azides are important in organic synthesis.[6] One of the most widely used reactions of aryl azides is the 1,3-dipolar cycloaddition reaction, in which a 1,3-dipole (in this case, an azide group) reacts with a dipolarophile:

Scheme 5- General 1,3-Dipolar Cycloaddition Reactions

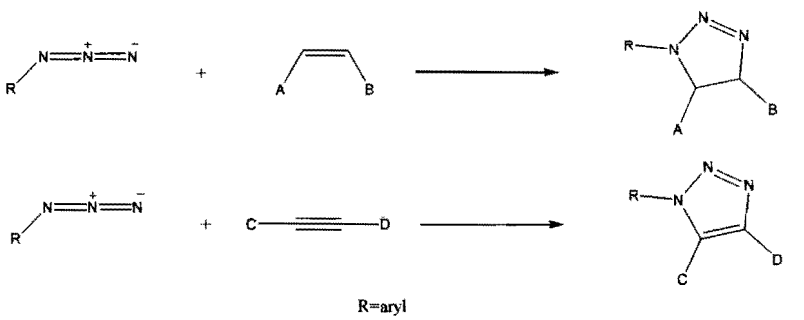

This type of reaction can be performed with both alkenes and alkynes. Most often, an azide is reacted with an alkyne using a copper I catalyst to give a substituted [1,2,3]-pyrrole.[7,41-46] This process has been used in the synthesis of peptidotriazoles,[7] bioconjugation,[42] cell-surface labeling,[45] and dendronization.[46]

Catalysis is not always necessary to promote this type of reaction. It was discovered in 1912 that alkenes are able to react with aryl azides to generate triazolines.[47] It was proposed that this reaction proceeds by a concerted mechanism,[48] and this has been supported by later studies.[49-51] The formation of the two new σ-bonds is concerted, leading to exclusive *cis*- addition products.[52] When the dipolarophile is asymmetric, the regioselectivity of the cycloaddition reaction is influenced by electronic effects: alkenes and alkynes bearing an electron-donating substituent preferentially form 5-substituted products, while those bearing electron-withdrawing groups form 4-substituted products.[53]

Figure 2- Regioselectivity of the Cycloadditions of Asymmetric Dipolarophiles

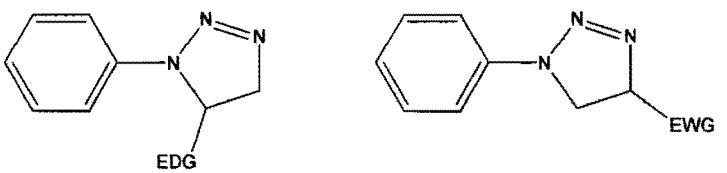

When the dipolarophile is an α,β- unsaturated ester, and the cycloaddition is carried out in the presence of base, a rearrangement to an open-chain diazo coumpound occurs. This species is also a 1,3- dipole, and therefore can undergo a second cycloaddition reaction to give a di-adduct.[54]

Scheme 6- Mechanism of Di-Adduct Formation

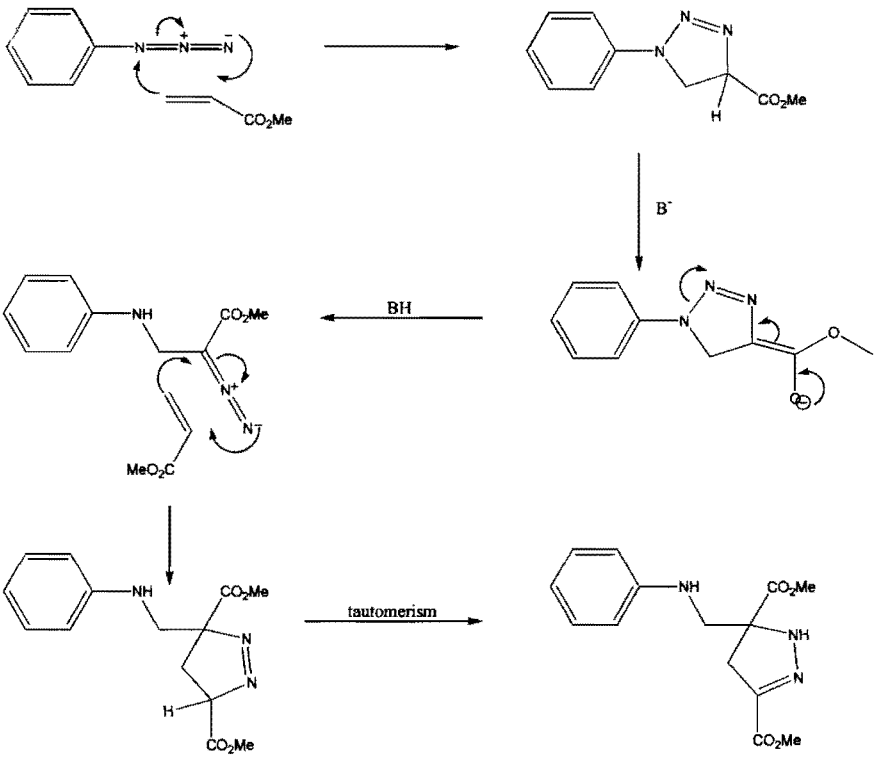

1.4- The Chemistry of Pyridyl Azides

1.4.1- Reactions Involving Nitrenes

Above, the chemistry of phenylnitrene was discussed at length. However, a slight change in the phenyl ring (replacement of a C-H unit with a nitrogen atom) can significantly alter the reactivity of the nitrene intermediates formed. Three isomeric forms of pyridyl nitrene exist: 2-, 3-, and 4-pyridyl nitrenes. 4-pyridyl nitrene behaves in the same manner as phenylnitrene,[55] so little attention will be paid to that species here.

2- and 3-pyridyl nitrene, however, may undergo different types of reactions than the parent phenylnitrene. 2-pyridyl nitrene undergoes rapid nitrogen scrambling via 1,3-diazacyclohepta-1,2,4,6-tetraenes:[56]

Scheme 7- Nitrogen Scrambling of 2-Pyridyl Nitrene

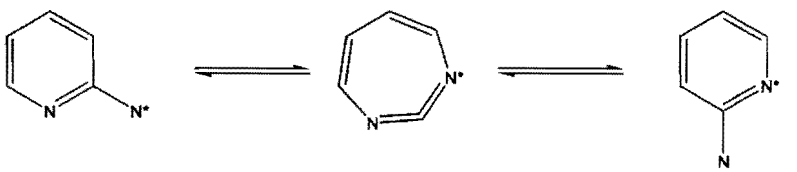

While unique, this type of reaction is also very similar to the singlet chemistry of phenylnitrene. Its end product, after a ring closure, is 2-cyanopyrrole.[55,56] However, 3-pyridyl nitrene may, in addition to the regular singlet rearrangement,[57] undergo a ring-opening reaction to give a nitrile ylide.[58]

Scheme 8- Ring-Opening of 3-Pyridyl Nitrene

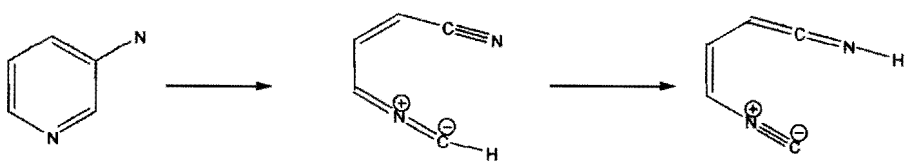

1.4.2- Formation of Tetrazoles from 2-Azidopyridine

A special reaction unique to 2-azidopyridine is its equilibrium isomerization to give tetrazolo[1,5-a]pyridine.[59] This species is interesting because of its contrasting nature as compared to the azide: the former is electronegative and the latter is electropositive. Calculated predictions indicate that in most cases (one exception is –COOH), the azide is stabilized when the pyridine ring is substituted with an electron-

withdrawing substituent, and the tetrazole is stabilized when an electron-donating group is substituted.[59]

Scheme 9- Tetrazole Formation from 2-Azidopyridine

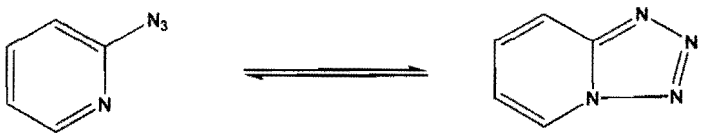

1.5- The Chemistry of Azidopyridine-1-Oxides

1.5.1- Reactions involving Nitrenopyridine-1-Oxides

The chemistry of nitrenopyridine-1-oxides is expected to be significantly affected by the back-donation of electrons from the oxygen atom into the pyridine ring.[60] Calculations indicate that all three isomers exist in their triplet ground states, and it has been suggested that the specific structure of 3-nitrenopyridine-1-oxide involves the distribution of the two unpaired electrons between the nitrene-N and the oxide-O centers,[60] which is said to account for its lower hydrogen-abstraction triplet reactivity.[61] In any case, both thermolysis and photolysis of all three azidopyridine-1-oxides resulted in complex product mixtures, and only the major products could be characterized.[61]

Recent laser flash photolysis experiments have shown that at room temperature, 4-nitrenopyridine-1-oxide undergoes intersystem crossing from the singlet state to the triplet state as the dominant process with k_{ISC}= 2.1 x 10^7 s^{-1}; no products arising from the singlet nitrene were observed in the study.[62] It is postulated that the complex product mixtures afforded in the previous studies could be attributed to photolysis of the primary

photoproduct [4,4'-azobis(pyridine-1-oxide)] of the reaction, and that the dominance of intersystem crossing at room temperature is due to the iminyl-cyclohexadienyl-aminoxyl character of the triplet nitrene (Figure 3).[62]

Figure 3- Resonance Contributors of Triplet 4-Nitrenopyridine-1-Oxide

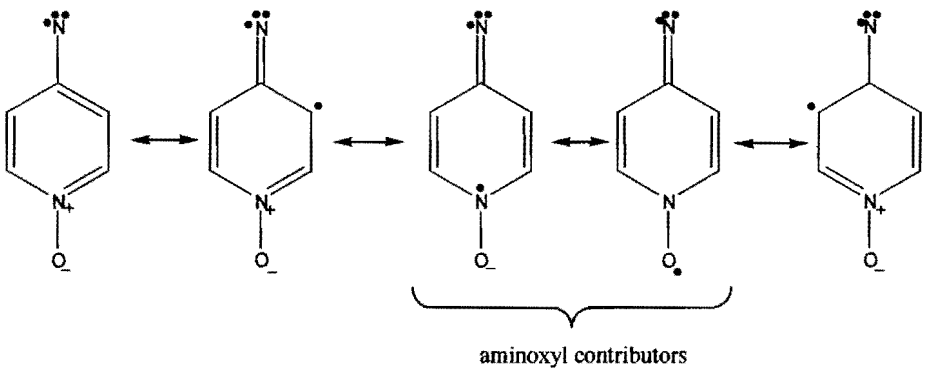

Other work with 2-azidopyridine-1-oxide shows that, in a manner similar to both phenylnitrene and 2-pyridyl nitrene, a rearrangement can occur to yield 1-hydroxy-2-cyanopyrrole.[63,64] It is unclear whether this reaction proceeds via a concerted ring opening followed by a ring closing or via a nitrene intermediate, but since the reaction proceeds under mild conditions and does not give other products indicative of nitrene chemistry, it is likely that it proceeds by the former.[64]

1.5.2- 1,3-Dipolar Cycloaddition Reactions of 4-Azidopyridine-1-Oxide

Like other aryl azides, 4-azidopyridine-1-oxide can undergo 1,3-dipolar cycloaddition reactions. However, unlike phenyl azide, which gives a pyrazole or pyrazoline product under normal conditions and a di-adduct in the presence of catalytic amounts of base, this compound may proceed directly to the di-adduct in the absence of base with some dipolarophiles.[65] It is unknown by what mechanism this reaction

proceeds; possibilities include 4-azidopyridine-1-oxide acting as its own base, the electronic structure of the compound causing a base to be unnecessary, or merely that the first step is rate-determining.[63]

1.6- Thesis Statement

The azidopyridine-1-oxides are interesting species due to their water solubility. This increases their usefulness in fields such as biochemistry, in which most reactions occur in an aqueous environment. It is possible that these species could be used as unique photoaffinity labeling reagents under more biologically meaningful conditions.

The ability of 4-azidopyridine-1-oxide to easily form a di-adduct with acrylates could potentially result in a new scaffold for dendrimer formation. The final product contains a pyrazine ring that, if cleaved and the ester groups hydrolyzed, would give four sites for protein growth. A protein grown on this scaffold would retain the strong chromophore endowed by the pyridine-1-oxide moiety, which could allow such a compound to be used as a chemosensor.

On a fundamental level, study of the effect of the 1-oxide group on the electronic structures, energetics, and reactivities of the nitrene species formed from photolysis of azidopyridine-1-oxides will provide new insight into the basic understanding of these concepts. In addition, determining the nature of the effect of the 1-oxide group on the cycloaddition chemistry of 4-azidopyridine-1-oxide will aid in the understanding of what effects it could have in more complex systems.

In order to achieve these studies, a number of experiments will be performed. Low-temperature photolysis and spectroscopy of 3- and 4-azidopyridine-1-oxide will be performed in various organic glasses in order to comparatively determine the effects of the 1-oxide group at different positions on the aromatic ring. In collaboration with Dr. Paul Lahti at the University of Massachusetts at Amherst, the electron paramagnetic resonance spectra of the nitrene intermediates formed by photolysis of these two compounds in organic glasses will also be performed. The product mixtures of these photolyses will be analyzed by high-pressure liquid chromatography (HPLC).

The 1,3-dipolar cycloaddition chemistry of 4-azidopyridine-1-oxide will be examined by performing a series of HPLC kinetic studies under varying conditions. By measuring the rate of disappearance of the parent azide and the rates of formation of the intermediates and products, insight about the mechanism and kinetic parameters of the reaction will be gained.

Chapter 2- Results and Discussion

2.1- The Photochemistry of 4-Azidopyridine-1-Oxide

2.1.1- Room Temperature Product Analysis

A 5 mM solution of 4-azidopyridine-1-oxide (7) in d_3-acetonitrile was photolyzed with multiple 266 nm pulses from a Nd-YAG laser. After photolysis, the sample was analyzed by high-pressure liquid chromatography. The following three-dimensional chromatogram was obtained:

Figure 4- HPLC PDA Output Following Photolysis of 4-Azidopyridine-1-Oxide

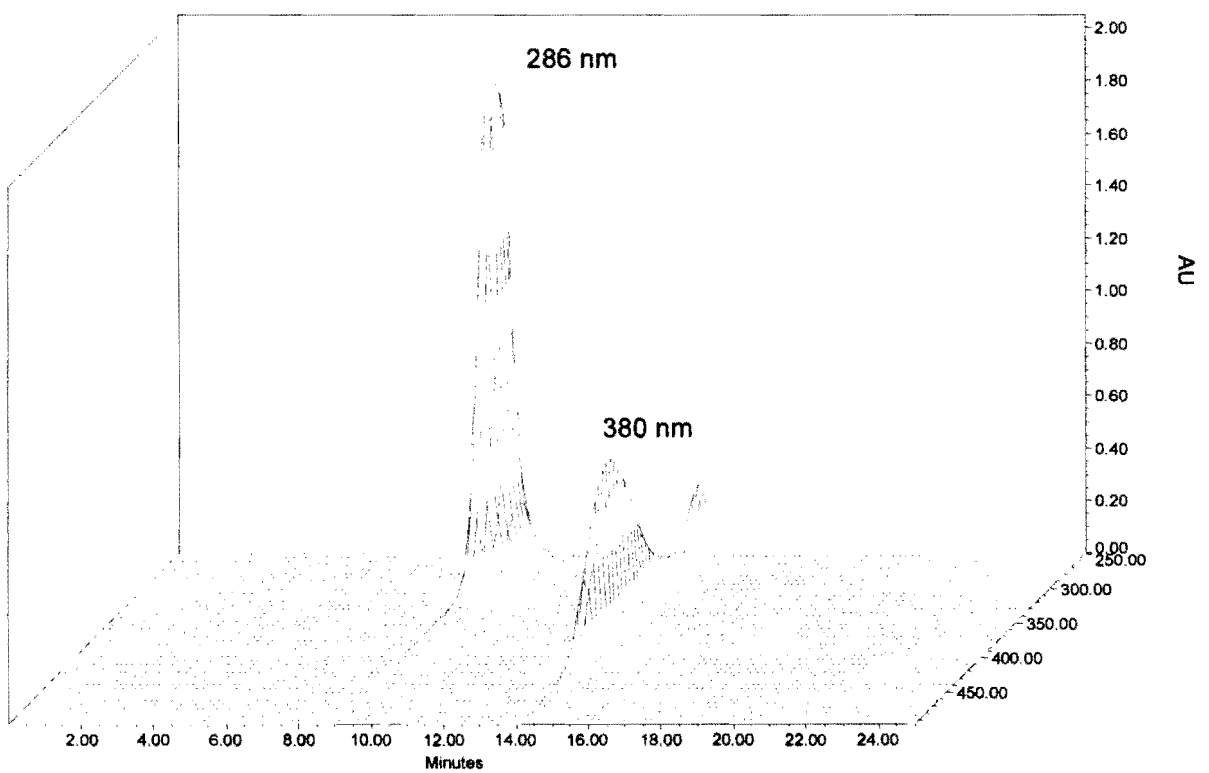

The first peak was assigned to residual **7**, and the second to 4,4'-azobis(pyridine-1-oxide) (**12**) on the basis of its peak absorbance. In order to confirm these assignments, an authentic sample of **12** was prepared and analyzed along with a sample of **7** under the same conditions. The resultant chromatogram was qualitatively similar to the chromatogram above.

Upon photolysis of **7**, molecular nitrogen and singlet 4-nitrenopyridine-1-oxide (^{1}**8**) are formed.[62] The reactions this species can undergo are analogous to those of phenyl nitrene, and are shown in Scheme 10.

Scheme 10- Reactions of 4-Nitrenopyridine-1-Oxide

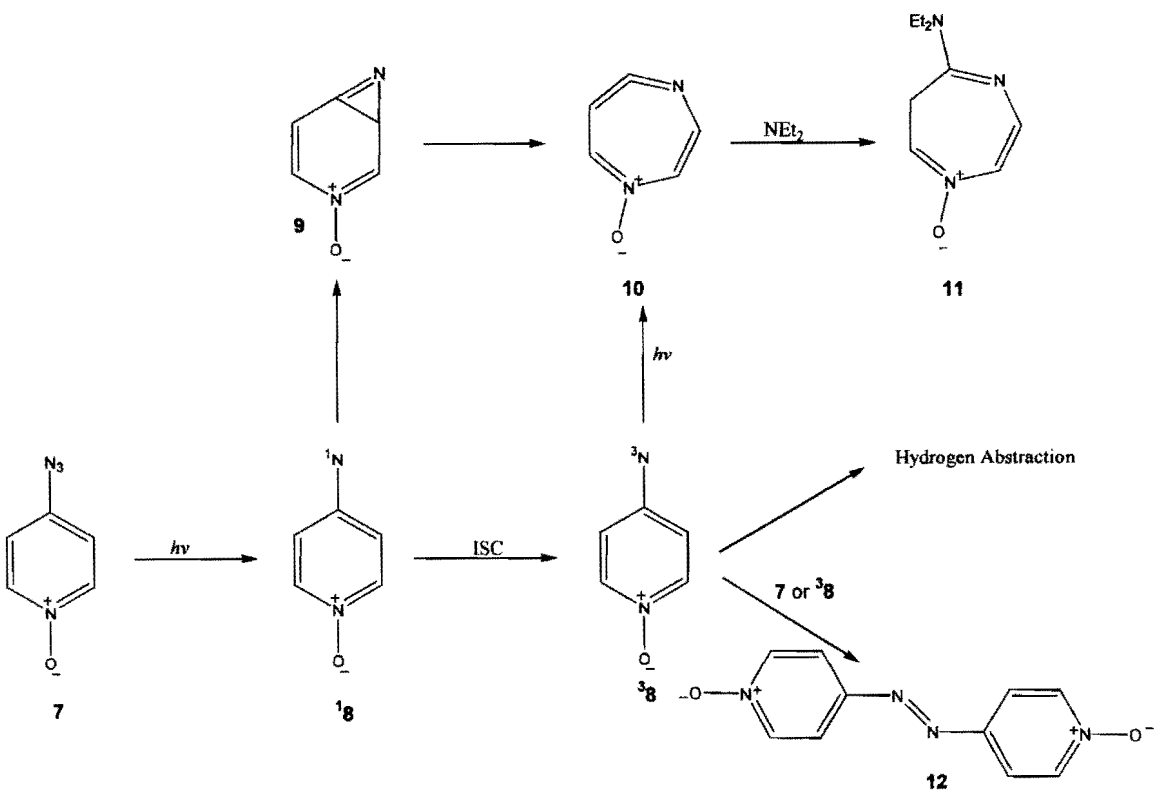

Since the HPLC chromatogram of the product mixture only shows one product, it is reasonable to assume that only one of these processes is dominant. Therefore, it was determined that intersystem crossing to the triplet (^{3}**8**) is the dominant process due to the presence of **12** alone in the product mixture. It is still unclear whether this species is formed by ^{3}**8** dimerization or by reaction of ^{3}**8** with **7**. Further experimentation is necessary to elucidate this.

As mentioned before, triplet nitrene species have been known to undergo hydrogen abstraction reactions with solvents. No evidence of this type of reaction was observed in d_3-acetonitrile; however, it was determined that for this particular system, reaction of ^{3}**8** to form **12** is diffusion-limited.[62] Therefore, in spite of the extremely large excess of solvent relative to **7** and ^{3}**8**, the barrier to hydrogen abstraction lowers the rate of that reaction enough relative to that of **12** formation to prevent its occurrence in this experiment. Furthermore, acetonitrile is a poor hydrogen donor. It is possible that hydrogen abstraction would occur more readily in a solvent more favorable to hydrogen donation, such as silanes or thiols.

2.1.2- Low-Temperature Studies

In order to more thoroughly probe the chemistry of ^{3}**8**, several types of low-temperature photolyses in glassy organic matrices at 77K were performed. One type of experiment was electron paramagnetic resonance (EPR) spectroscopy, which was performed by Dr. Paul Lahti at the University of Massachusetts at Amherst in glassy ethanol and 2-methyltetrahydrofuran (2-mTHF). The other low-temperature experiment was photolysis of **7** in glassy 3-methylpentane (3-MP) and 2-mTHF, followed by HPLC

and NMR analysis of the thawed product mixtures. Both of these experiments were also performed with samples of 3-azidopyridine-1-oxide (**13**) for comparison. The reactions this species can undergo after photolysis to give singlet 3-nitrenopyridine-1-oxide (^{1}**14**) are shown in Scheme 11.

Scheme 11- Reactions of 3-Nitrenopyridine-1-Oxide

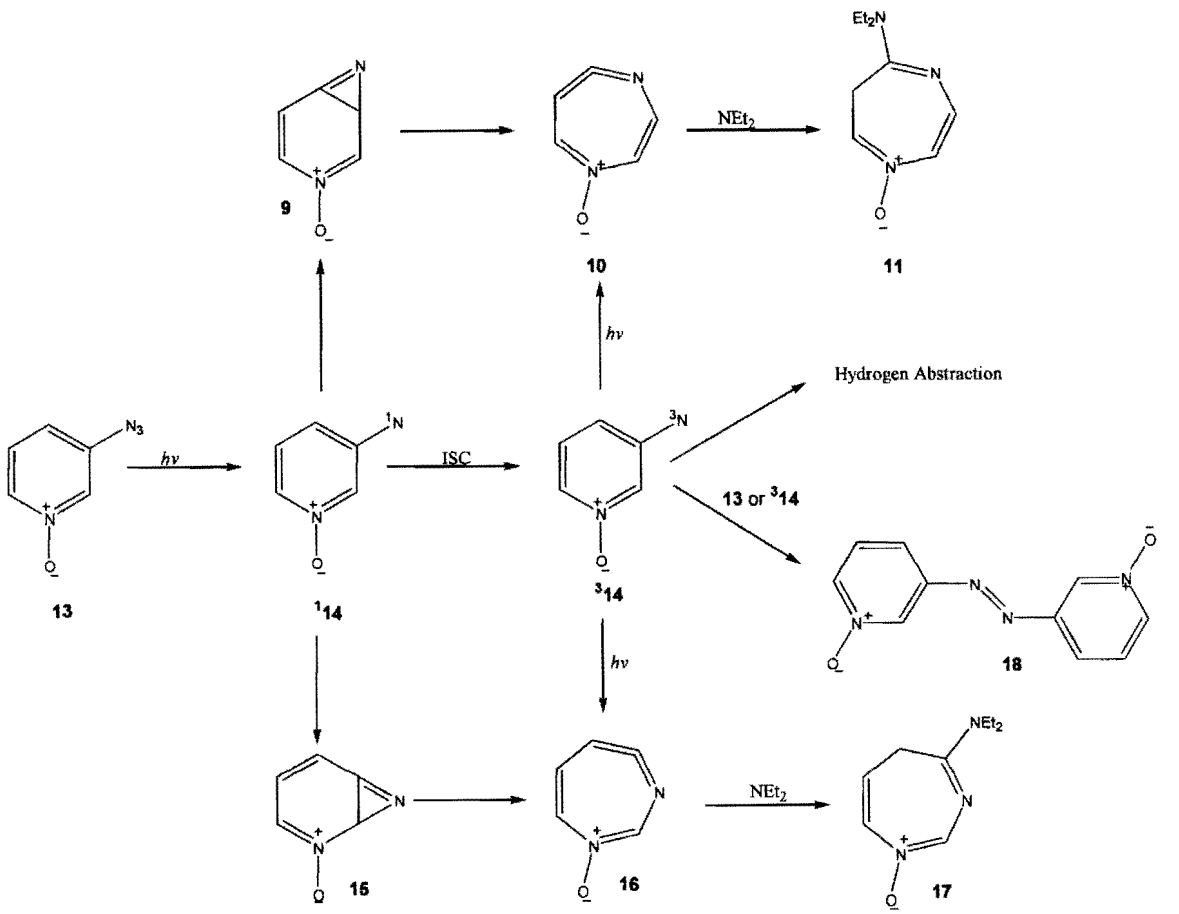

Photolysis of **7** and **13** in glassy ethanol gave the EPR spectra shown in figure 5.

Figure 5- EPR Spectra of 3- and 4-Nitrenopyridine-1-Oxide in Ethanol at 77K

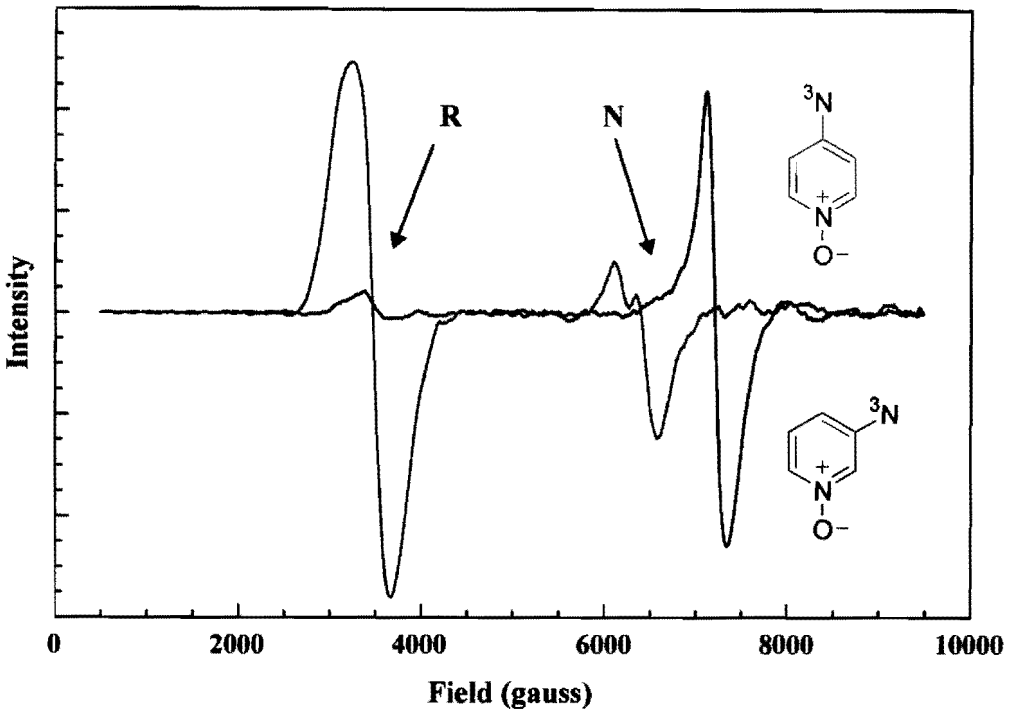

Since EPR spectra only detect unpaired electrons, only triplet species will be detected, as it will be recalled that the spins of open-shell singlet electrons are opposite. The EPR spectrum of ^{3}**14** (shown in black) exhibits $|D/hc|$= 1.089 cm^{-1} with $|E/hc| \leq$ 0.003 cm^{-1}.

The EPR spectrum of ^{3}**8** is much more interesting. In addition to a strong signal indicative of adventitious radical species, it appears that two unique nitrene signals are present. The first, presumably the signal owing to the presence of ^{3}**8**, exhibits $|D/hc|$= 0.790 cm^{-1} with $|E/hc| \leq$ 0.004 cm^{-1}. The significantly lower value for $|D/hc|$ for this species relative to that of ^{3}**14** as well as the analogous 4-nitrenopyridine ($|D/hc|$= 1.107 cm^{-1} with $|E/hc| \sim$ 0 cm^{-1})[66] is indicative of a high degree of spin delocalization. Most likely, this spin is delocalized in large part on the oxygen atom of ^{3}**8**, as is consistent with the calculated Natural Population Analysis for that species.[62] The second nitrene signal

was unexpected, and initial low-temperature photolysis experiments in 3-MP did not detect a signal indicative of a second nitrene species[65].

Because of these results, further low-temperature experiments were performed. A typical experiment is as follows: a solution of the azide precursor in the appropriate solvent was prepared such that its peak UV/Vis absorbance was between 1.5 and 2. The solution was then immersed in liquid nitrogen and a glass was allowed to form. A spectrum was taken upon glass formation. Then, photolysis with a medium-pressure Hg-vapor lamp was performed at certain time intervals, and a spectrum taken after each. Upon completion of photolysis, the solution was allowed to thaw, at which time it was refrozen and a spectrum taken. Finally, the solution was allowed to thaw again, and a final room-temperature spectrum taken. The product mixture was then analyzed by HPLC.

More concentrated samples were then photolyzed in order to obtain sufficient material for NMR analysis. In such an experiment, a concentrated solution of the appropriate azide in 3-MP was frozen at 77K and photolyzed for approximately 1600 seconds with a medium-pressure Hg vapor lamp. This process was repeated multiple times. The thawed product mixtures were combined and extracted with D_2O, then analyzed by ^1H NMR.

Photolysis of **13** in 3-MP and 2-mTHF gave the baseline-corrected spectra shown in Figure 6. The thawed and revitrified spectra are shown offset.

Figure 6- UV/Vis Spectra: Photolysis of 3-Azidopyridine-1-Oxide in 2-Methyltetrahydrofuran (Top) and 3-Methylpentane (Bottom) Glasses at 77K

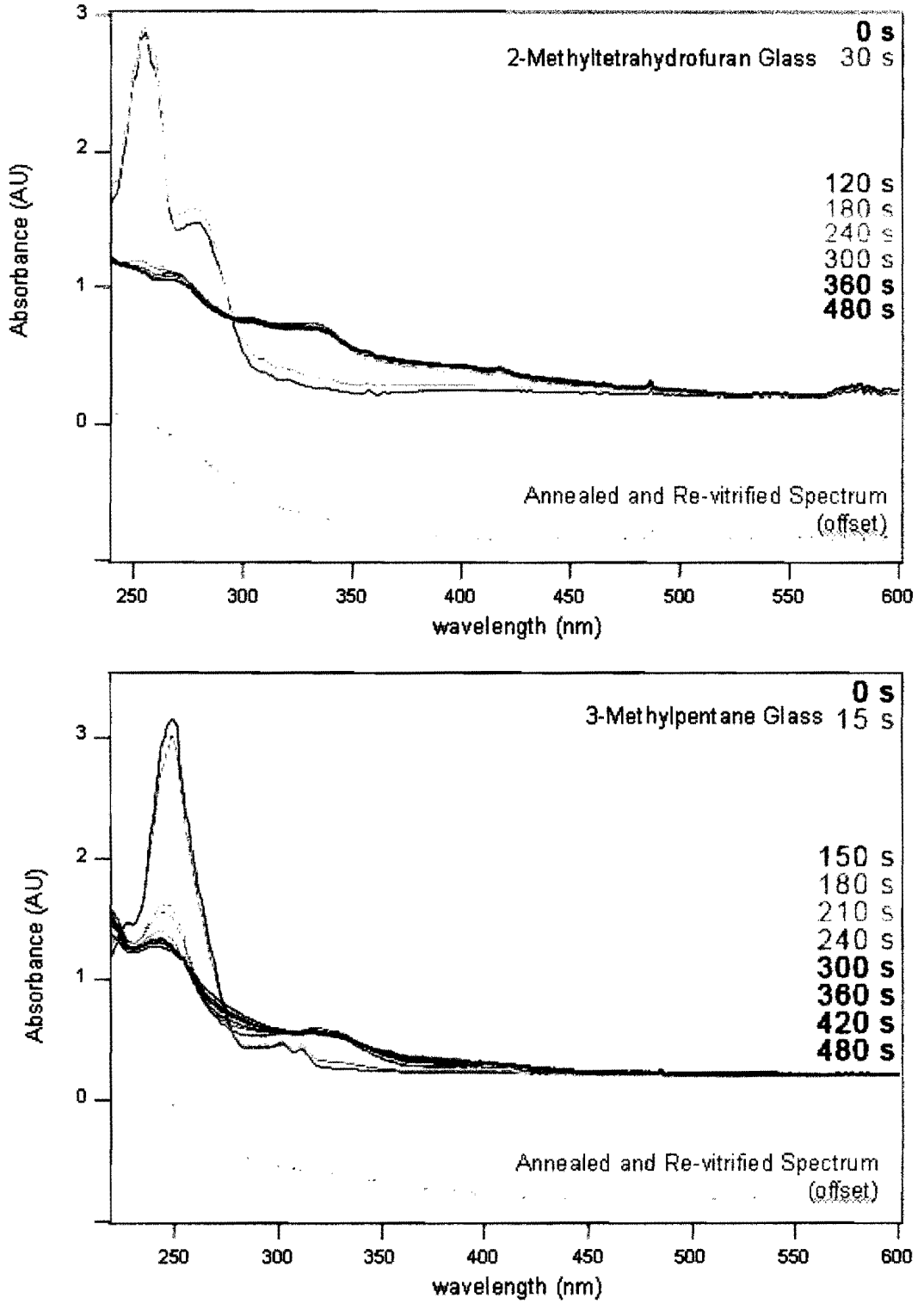

In both solvents, a broad, unstructured feature grows in the 300-350 nm range, accompanied by gradual weakening of the signal at around 280 nm, which corresponds to the starting azide **13**. The former of these is consistent with other triplet arylnitrenes, and so it has been assigned to ^{3}**14**. As was shown in Scheme 11, this species can undergo a number of different types of reactions. It can absorb another photon of light to form either **10** or **16**, which, in the absence of a nucleophilic trap, would polymerize upon thawing. It could also undergo hydrogen abstraction with the solvent, or react to give **18**.

HPLC analysis of the product mixture of the photolysis of **13** in 2-mTHF was unhelpful, since after multiple analyses no signals could be readily distinguished from instrument noise. However, the product mixture arising from photolysis in 3-MP gave one predominant signal with a retention time different from that of **13** (Figure 7). The presence of only one signal is interesting, as it suggests that little competition exists among the multiple pathways.

NMR analysis of the product mixture suggested that hydrogen abstraction from the solvent followed by coupling with the radical formed was the dominant process. In the aromatic region (Figure 8), two multiplets corresponding to **13** can be seen at about 7.58 and 8.12 ppm. In that region are also found smaller signals, including an apparent singlet at 8.51, two doublets at 8.50 and 8.27, and a feature similar to a doublet of doublets at 8.21 ppm. This combination of signals is suggestive of a 3-substituted pyridine-1-oxide distinct from the parent compound, as each integrates to approximately one hydrogen atom. In the alkyl region (Figure 9), among other features can be seen a quartet-like feature at 1.53 ppm which integrates to roughly four hydrogen atoms, a singlet at 1.11 ppm which integrates to roughly three, and a triplet feature at 0.83 ppm

that cannot be reliably integrated due to underlying signals. This set of signals seems to correspond to a 3-substituted-3-methylpentyl group. From this information, it is likely that 3-(N-[1'-ethyl-1'-methylpropyl])aminopyridine-1-oxide is the dominant photoproduct following photolysis of **13** in 3-MP glass at 77K. This assignment is reasonable due to the lower energy barrier to hydrogen abstraction from a tertiary carbon atom than from a primary or secondary carbon in an alkane.

Figure 7- HPLC PDA Output Following Photolysis of 3-Azidopyridine-1-Oxide in 3-Methylpentane Glass at 77K

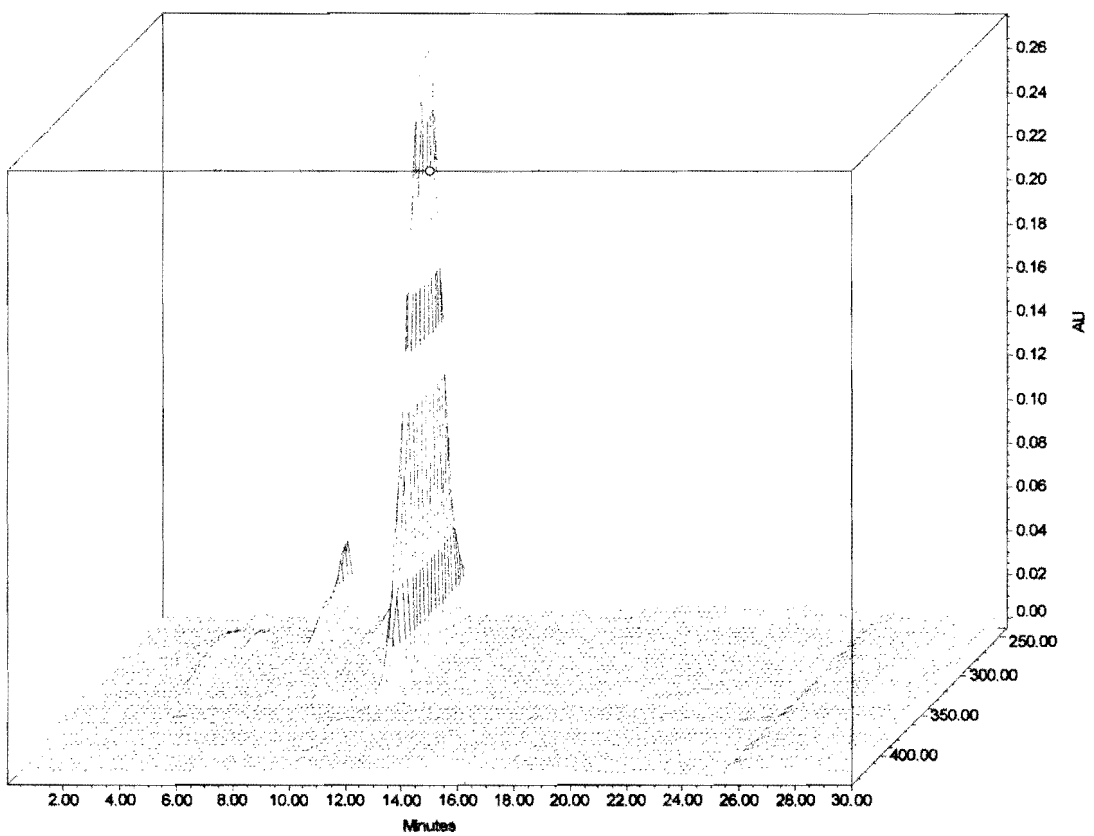

Figure 8- Aromatic Region of ^1H NMR Spectrum (D_2O) Following Photolysis of 3-Azidopyridine-1-Oxide in 3-Methylpentane Glass at 77K

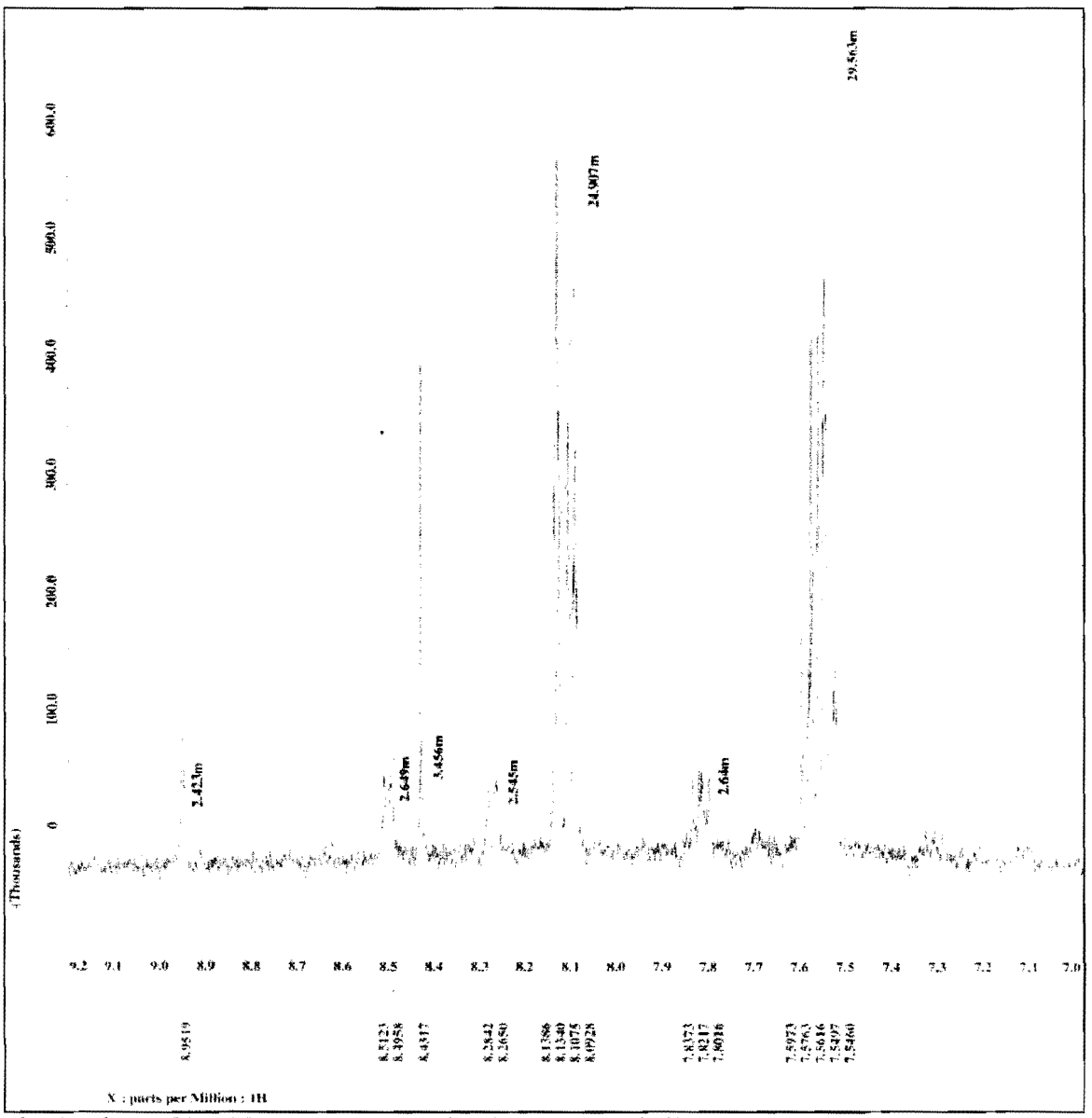

The signals at 7.56 and 8.12 ppm correspond to the starting azide (**13**).

Figure 9- Alkyl Region of ^1H NMR Spectrum (D_2O) Following Photolysis of 3-Azidopyridine-1-Oxide in 3-Methylpentane Glass at 77K

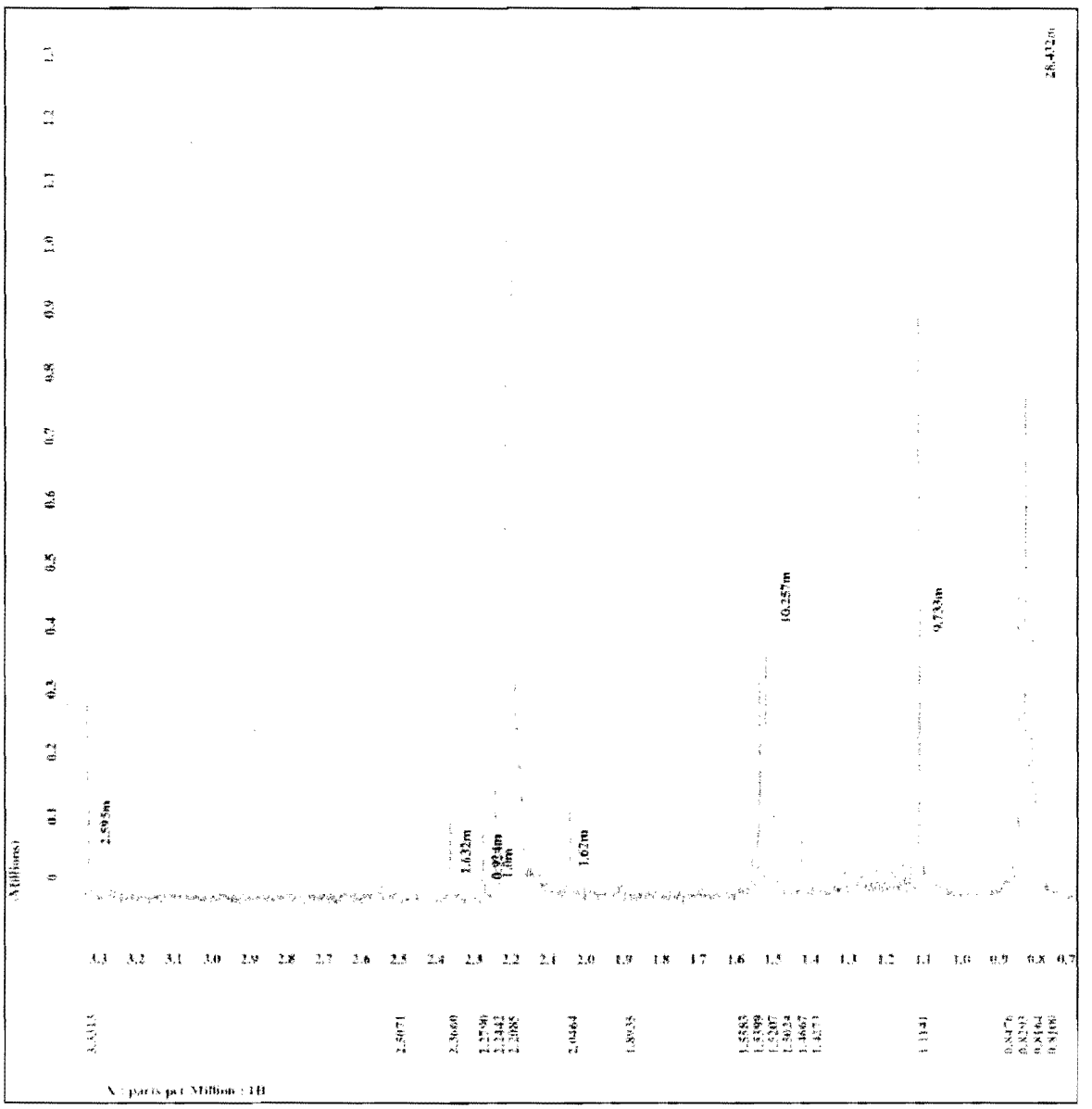

Photolysis of **7** in the same two solvents gave the baseline-corrected spectra shown in Figure 10.

Figure 10- UV/Vis Spectra: Photolysis of 4-Azidopyridine-1-Oxide in 2-Methyltetrahydrofuran (Top) and 3-Methylpentane (Bottom) Glasses at 77K

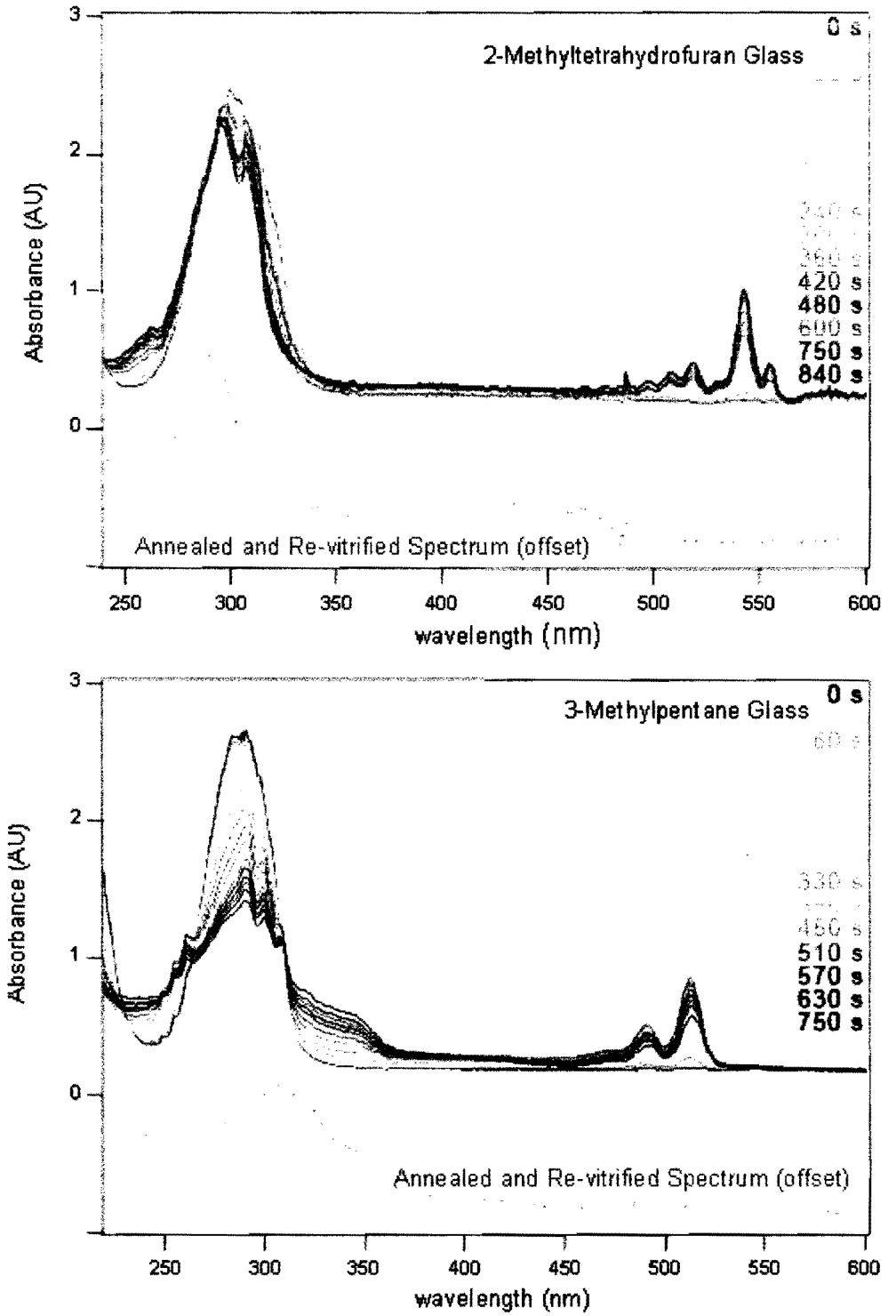

In 3-MP, ^{3}**8** appears as a structured series of bands at 500-520 nm, and the starting azide **7** has a peak absorbance around 290 nm. Midway through photolysis, the intensity of the signal corresponding to ^{3}**8** stops increasing and begins to decrease as a new broad feature grows at 320-360 nm. Upon thawing, the triplet signal is extinguished as expected. The possible fates of the nitrene formed upon photolysis of **7** were shown in Scheme 10. Evidence from the EPR spectrum and previous experiments[62] suggest that singlet reactions are unlikely, and that prolonged photolysis of ^{3}**8** is unlikely to give **10**. The product cannot be **12**, since the new signal grows in while the system remains glassy, and the maximum wavelength of the new signal is inconsistent with that of **12**. Therefore, the product is most likely the result of hydrogen abstraction from the solvent.

HPLC analysis of the product mixture shows only one product (Figure 11). Although its retention time is similar to that of **7**, the maximum wavelength is sufficiently different to eliminate **7** from consideration. Due to the lower barrier to hydrogen abstraction from a tertiary carbon as mentioned above, it is likely that the final product of such a reaction would be 4-(*N*-[1'-ethyl-1'-methylpropyl])aminopyridine-1-oxide.

NMR analysis following photolysis of a more concentrated solution was more complex. The aromatic region (Figure 12) showed features corresponding to **7** (d, 8.23; d, 7.28) and **12** (d, 8.52; d, 8.11), in addition to the major photoproduct(s). One set of doublets at 8.35 and 6.75 ppm (J= 7.3 Hz for each) can be seen, as well as another set of signals at 7.84 (d, J= 7.0 Hz) and 8.52 ppm (most likely a doublet overlapping with that of **12**). A number of minor signals were also observed. In the alkyl region (Figure 13), the same quartet-singlet-triplet pattern as observed in Figure 9 can be seen, which is indicative of the previously mentioned 3-substituted-3-methylpenyl moiety. Therefore, it

is reasonable to assume that 4-(*N*-[1'-ethyl-1'-methylpropyl])aminopyridine-1-oxide is one of the major photoproducts following photolysis of a concentrated solution of **7** in 3-MP, and may be the compound responsible for the HPLC signal in Figure 11.

Figure 11- HPLC PDA Output Following Photolysis of 4-Azidopyridine-1-Oxide in 3-Methylpentane Glass at 77K

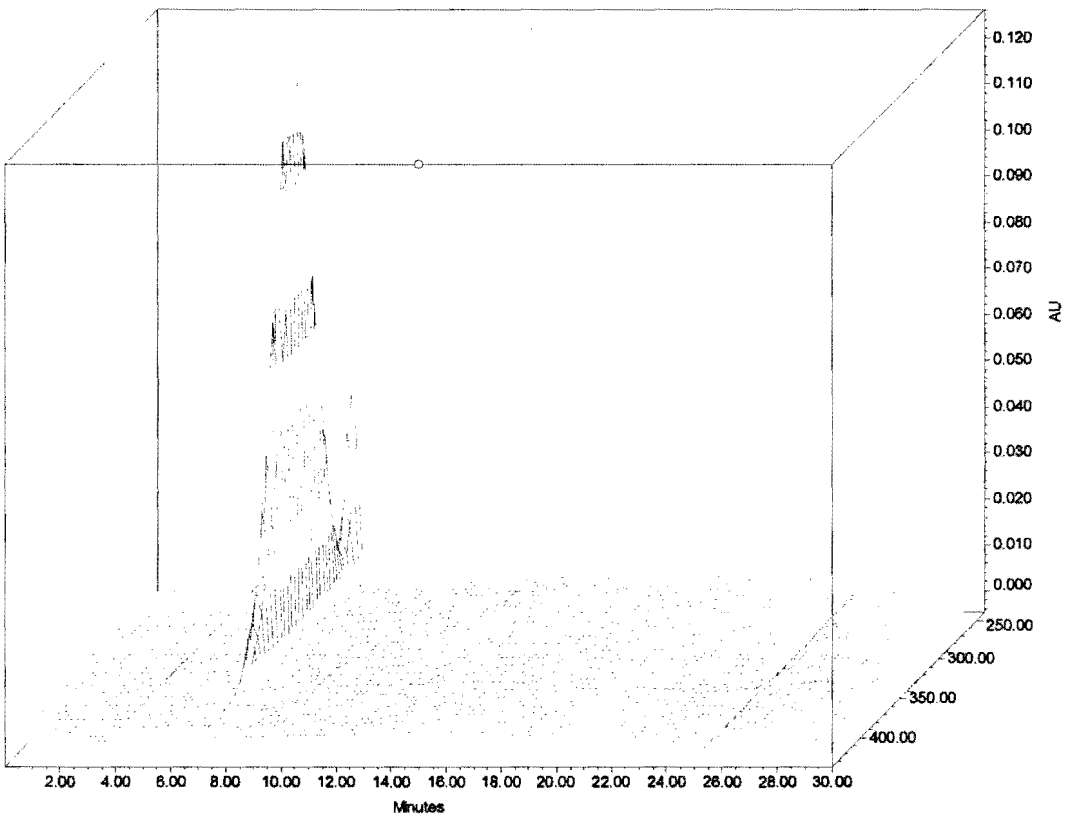

A different result was observed when **7** was photolyzed under the same conditions in 2-mTHF. In this case, two sets of structured bands appear, one around 500-520 nm, and the other around 540-560 nm. These signals appear simultaneously; therefore, one is not the product of a reaction involving the other. Also of interest is that both signals seem to hit a growth plateau after a certain period of time. This is different from the experiment

Figure 12- Aromatic Region of ^{1}H NMR Spectrum (D_2O) Following Photolysis of 4-Azidopyridine-1-Oxide in 3-Methylpentane Glass at 77K

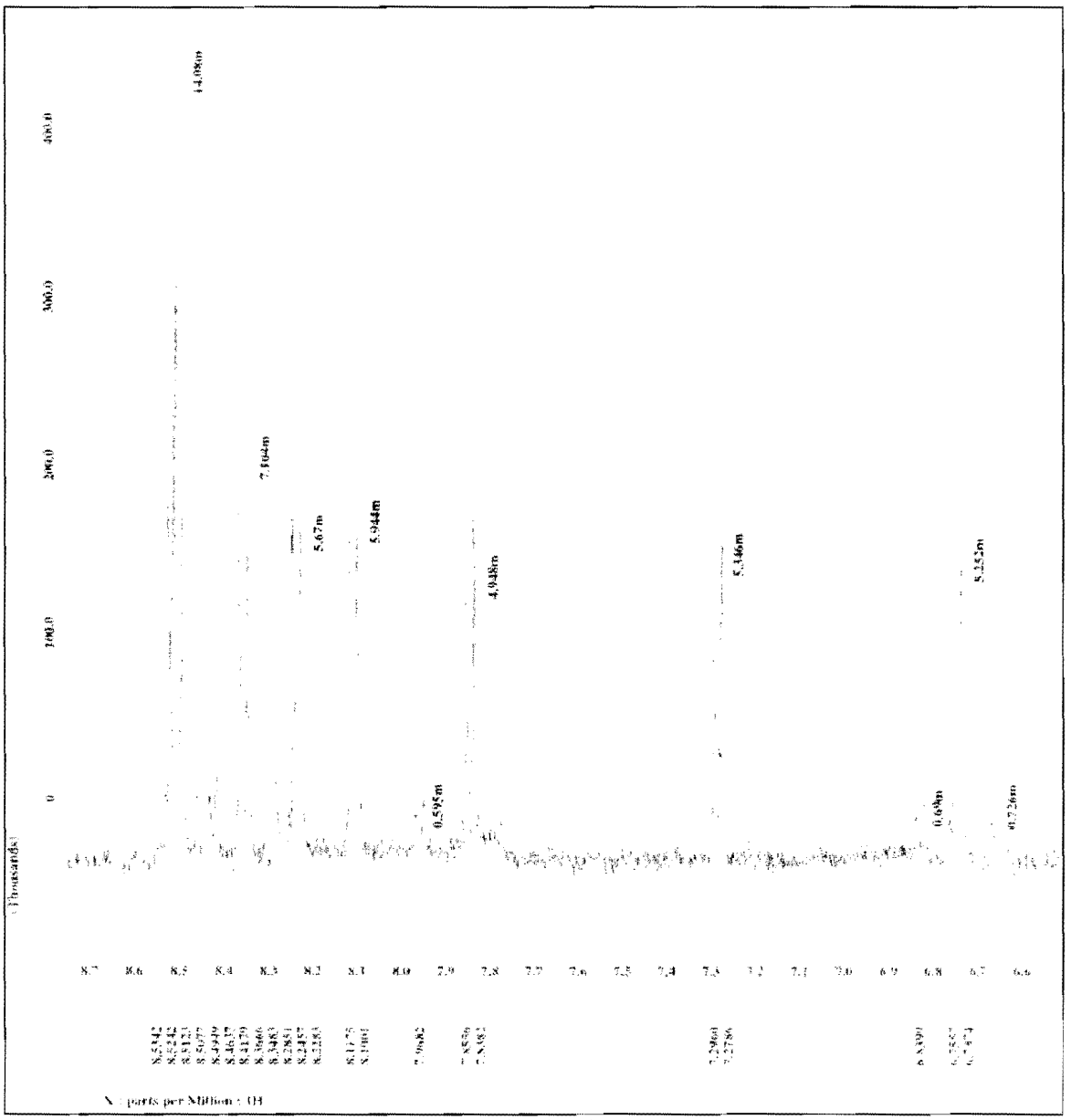

The signals at 7.28 and 8.23 ppm correspond to 7; the signals at 8.11 and 8.51 ppm correspond to **12**..

Figure 13- Alkyl Region of ^{1}H NMR Spectrum (D_2O) Following Photolysis of 4-Azidopyridine-1-Oxide in 3-Methylpentane Glass at 77K

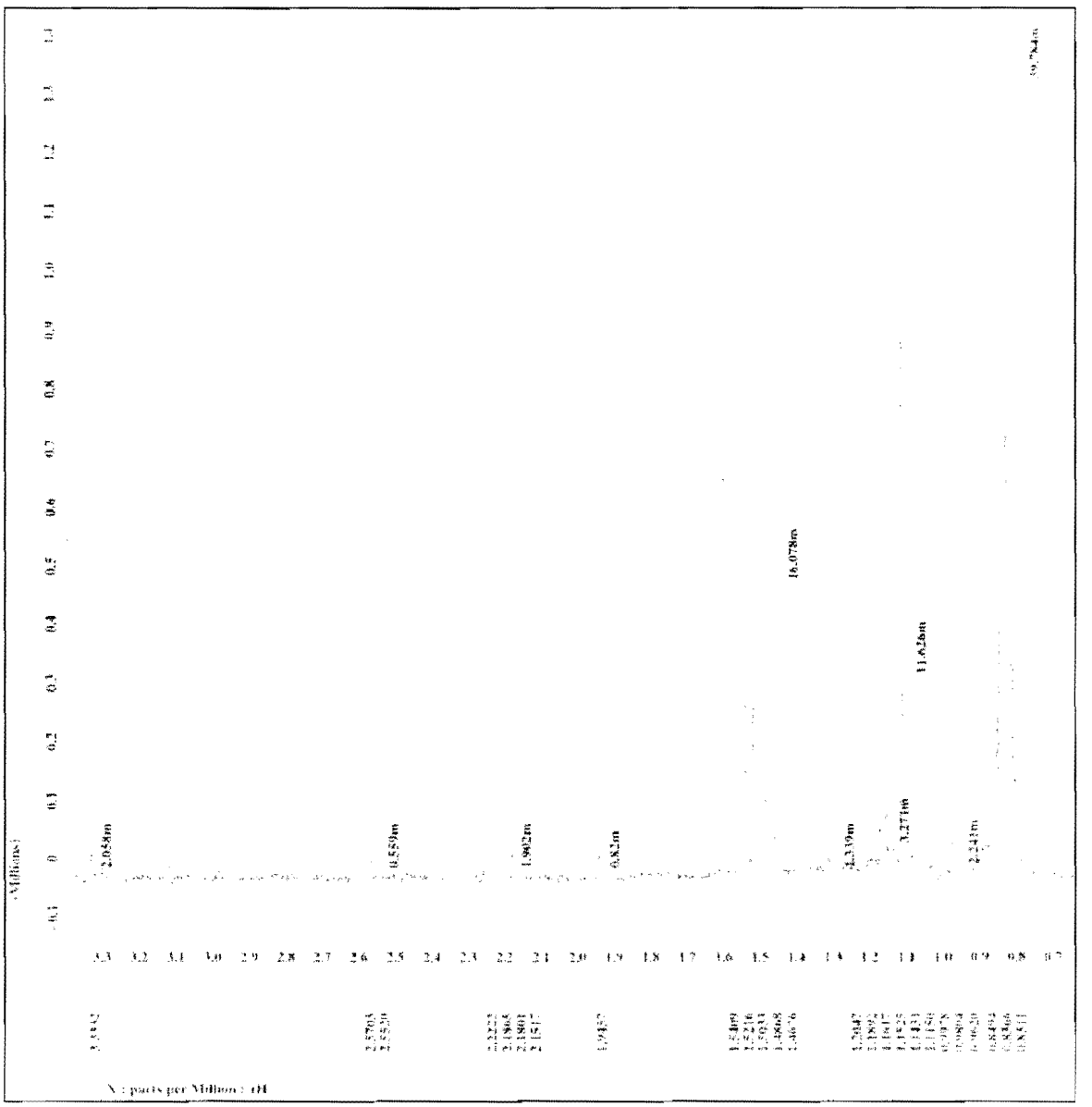

conducted in 3-MP, in which the signal at 500-520 nm began to decrease concurrently with an increase in absorbance elsewhere. No definitive assignments to these signals can be made at this time, except that at least one of them corresponds to ^{3}**8**. It is possible that

one signal corresponds to ^{3}**8** and the other to a second unknown nitrene species as might have been suggested by the EPR spectrum in ethanol. However, it is also possible that both sets of signals correspond to the same species. Upon thawing, both sets of signals vanish.

HPLC analysis of the product mixture was not helpful. A number of signals are detected; one corresponds to residual **7** and one to **12** based on their retention times and spectral characteristics. In most cases, however, it is difficult to determine whether the signal corresponds to an actual product or if it is merely a figment of instrument noise. LC/MS experiments would begin to aid in the identification of these products. At present, the only conclusion that can be drawn is that the properties of the solvent seem to have a strong effect on the reactivity of the nitrene species formed.

2.2- Kinetic Studies: 1,3-Dipolar Cycloaddition Reaction of 4-Azidopyridine-1-Oxide with Methyl Acrylate

In order to study the 1.3-dipolar cycloaddition reaction mechanism of **7**, a series of kinetic experiments with methyl acrylate were performed. An explanation of the experimental details can be found in Section 3.3.5. HPLC analysis of the aliquots taken showed as many as seven unique signals, which have been assigned as follows: 7.4 min.: Unknown 1, 7.8 min.: **7**, 8.9 min.: Unknown #2, 10.1 min.: 4-[1'-(4'-methoxycarbonyl)-1',2',3'-triazolinyl]pyridine-1-oxide (monoadduct), 11.3 min.: *N*'-[5'-(3',5'-dimethoxycarbonyl)-4',5'*H*-dihydroxypyrazolyl)methyl-4-aminopyridine-1-oxide (diadduct), 14.4 min.: methyl acrylate, 20.2 min.: methyl benzoate (internal standard).

The general trend observed in the majority of kinetic runs was that consumption of **7** led to rapid formation of the diadduct. Formation of what is assumed to be the monoadduct was not observed until later in the run, and generally remained at about a steady concentration. The assignment of this peak as the monoaduct is based on its similarity to a classical steady-state intermediate according to its rate of formation during the run. After a certain point in each run, however, the diadduct concentration rapidly dropped, and a new peak formed corresponding to unknown #1. Attempts to characterize this species by ^{1}H NMR of the product mixture were unsuccessful, and at present no assignment to this species can be made. The drop in concentration of the diadduct is due at least in part to a solubility issue; at a certain point the concentration reaches a supersaturated level at which time crystallization rapidly occurs. This does not rule out the possibility of a decomposition leading to the formation of unknown #1. In some runs, another unknown peak (unknown #2) was observed to grow in and then fade away during the course of the run; it is also currently unknown what this species may be. These general trends are best seen in Figure 14.

Pseudo first-order treatment of the rate of reactions in varying concentrations of methyl acrylate, measured as the rate of the disappearance of **7** yielded the graph shown in Figure 15. Linear regression analysis of the data yielded the second-order rate coefficient k_{cyc} 1.00×10^{-5} $M^{-1}s^{-1}$, in good agreement with previous studies.[65]

From these data, a few conclusions about the nature of the mechanism can be drawn. First, the overall process is not concerted. This fact is evidenced by the observation that formation of the diadduct requires two equivalents of methyl acrylate, which would cause the rate of reaction to be second order in this species. Since it is only

first order in methyl acrylate, the mechanism must proceed in a stepwise manner. It can also be concluded that the first cyclization to yield the monoadduct is the rate-determining step, and that all other steps in the mechanism are relatively fast. Therefore, if the mechanism shown in Scheme 6 is similar to that for this system (excluding the presence of base), the energy barrier for the step leading to the ring-opening of the monoadduct must be lower than that observed for simple phenyl azides, which require base catalysis. Whether this is due to internal electronic effects or self-catalysis remains unknown at present.

Figure 14- Variation of Product Distribution over Time: Kinetic Run #7

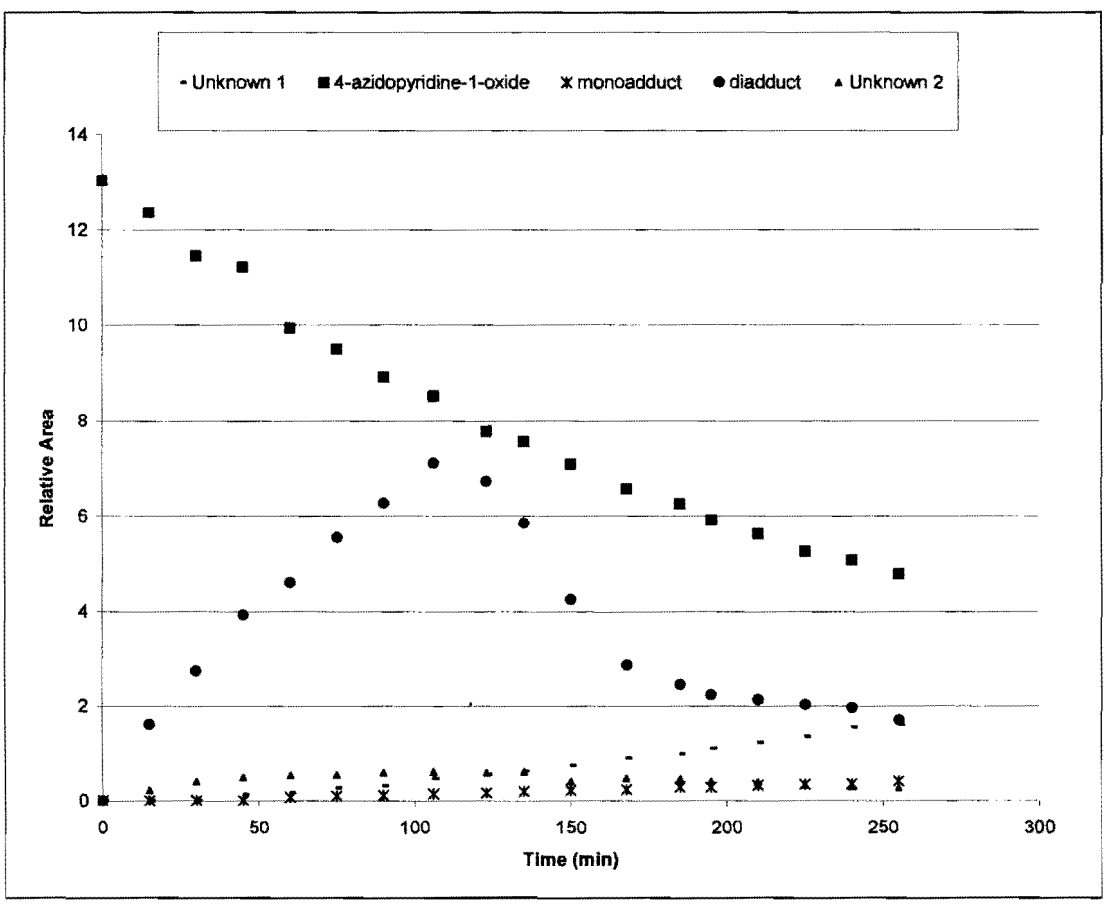

Figure 15- Pseudo First-Order Treatment of 1,3-Dipolar Cycloaddition Reaction of 4-Azidopyridine-1-Oxide with Methyl Acrylate

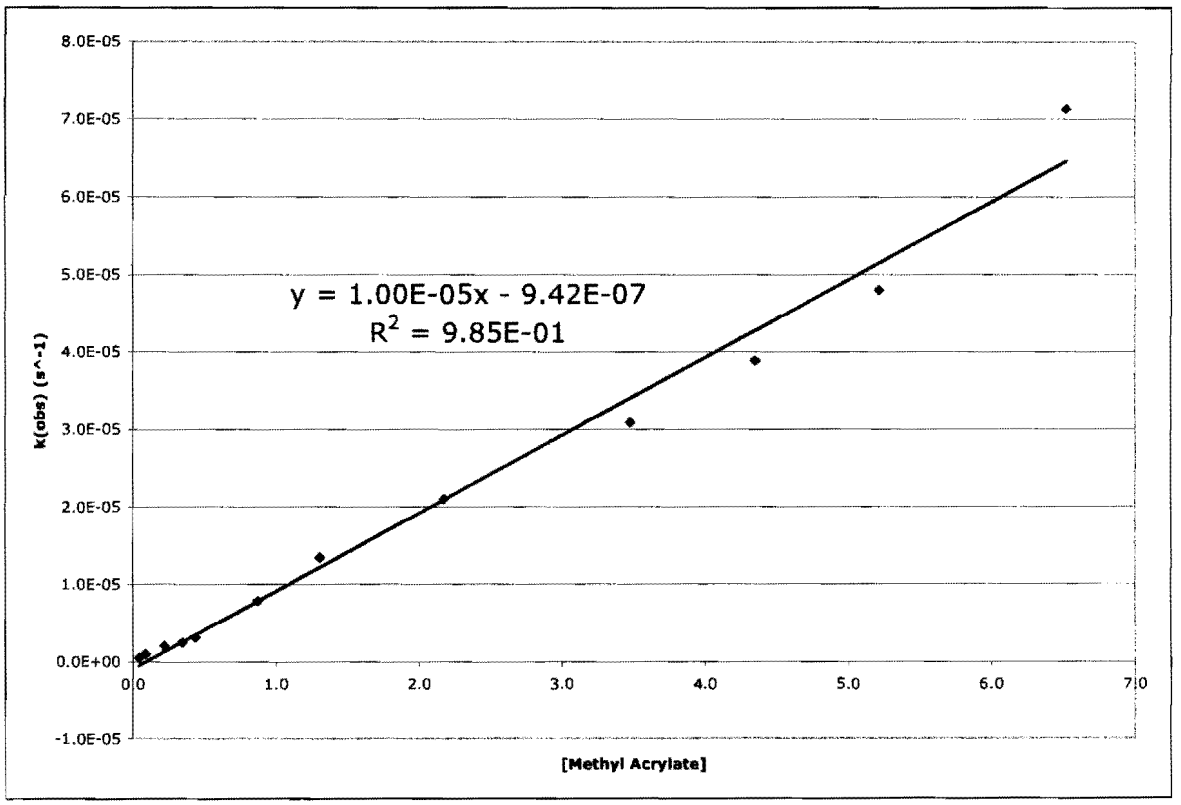

Chapter 3- Experimental Details

3.1- Materials

Materials were purchased from commercial sources and used without further purification with the exception of methyl acrylate, which was distilled prior to use in kinetic studies.

3.2- Instrumentation

IR spectra were obtained on a Perkin-Elmer FT-IR Spectrometer- Spectrum 100. NMR spectra were obtained on a 400MHz JEOL Eclipse 400 Multinuclear NMR Spectrometer. UV/Visible spectra were obtained on an Agilent 8453 Photodiode Array Spectrophotometer.

High Performance Liquid Chromatography was performed with a Waters 2695 Separations Module attached to a Waters 2996 Photodiode Array Detector with an Alltech Alltima C-18 3μ 4.6 mm i.d. x 150 mm column.

3.3- Experimental Methods

3.3.1- Preparation of 4-Chloropyridine-1-Oxide by the Method of Ochai[67]

To 10.02g (71.5 mmol) of 4-nitropyridine-1-oxide were added 60 mL (800 mmol) of acetyl chloride. The resultant mixture was heated to reflux at 50° C with stirring for about 45 minutes, at which time the evolution of brown gas (NO_2) appeared to cease (the formed NO_2 was trapped with water away from the reaction vessel). The excess acetyl

chloride was immediately removed by distillation, and the resultant mixture carefully made basic with sat. Na_2CO_3 solution. This basic solution was then extracted with chloroform (7 x 100mL), dried (Na_2SO_4), and stripped of solvent by rotary evaporation. The residue was recrystallized from acetone and the crystals collected by vacuum filtration to give 7.47g (57.6 mmol; 81%) of 4-chloropyridine-1-oxide.

^{1}H NMR ($CDCl_3$; 400 MHz): δ= 8.20 (d, J= 7.0 Hz, 2H); 7.32 (d, J= 7.0 Hz, 2H) ppm.

3.3.2- Preparation of 4-Hydrazinopyridine-1-Oxide by the Method of Katritzky[68]

2.52g (19.4 mmol) of 4-chloropyridine-1-oxide and 8.8mL (180 mmol) of hydrazine monohydrate were combined and set to reflux at 105° C with stirring for 30 minutes. The reaction vessel was then immediately removed from heat, sealed, and placed into a freezer overnight. The mixture was then vacuum filtered to give 1.94g (15.5 mmol; 80%) of 4-hydrazinopyridine-1-oxide, which was used without further purification. Yields ranged from 80-84%.

3.3.3- Preparation of 4-Azidopyridine-1-Oxide by the Method of Sawanishi *et. al.*[57]

To a stirring solution of 1.94g (15.5 mmol) of 4-hydrazinopyridine-1-oxide in 15mL of 5% HCl in an ice bath was added dropwise a solution of 1.12g (16.2 mmol) of $NaNO_2$ in 12mL of distilled water. Upon completion of the addition, the solution was removed from the ice bath and allowed to stir at room temperature for 30 minutes. The solution was then made basic with sat. Na_2CO_3 solution and combined with two other batches of similarly treated 4-hydrazinopyridine-1-oxide (total: 5.74g; 45.8 mmol). The combined basic solutions were extracted with chloroform (10 x 50mL), dried (Na_2SO_4), and

stripped of solvent by rotary evaporation. The residue was recrystallized from acetone and the resultant crystals harvested by vacuum filtration to give 2.71g (20.0 mmol; 44%) of 4-azidopyridine-1-oxide.

^{1}H NMR ($CDCl_3$; 400Mhz): δ= 8.35 (d, J= 7.7 Hz, 2H); 7.05 (d, J= 7.3 Hz, 2H) ppm.

^{13}C NMR ($CDCl_3$; 100MHz): δ= 140.4 (C_2); 138.8 (C_4); 116.6 (C_3) ppm.

IR ($CDCl_3$): υ= 2124, 2096 ($-N_{3\ str.}$) cm^{-1}.

UV-Vis (CH_2Cl_2): λ_{max} ($\log_{10}\varepsilon$)= 304 (4.26) nm.

UV-Vis (CH_3CN): λ_{max} ($\log_{10}\varepsilon$)= 302 (4.35) nm.

MS (Electrospray): $C_5H_5N_4O$ (M+H) required= 137.0643; actual= 137.0457

3.3.4- Preparation of 4,4'-Azobis(pyridine-1-oxide) by the Method of Muniz-Miranda *et. al.*[69]

71.4 mL of a 0.1M solution of $NaBH_4$ was added dropwise over a period of 1 hour to 71.4 mL of a 0.1M solution of 4-nitropyridine-1-oxide. The solution was stirred at room temperature for 24 hours. It was then stripped of solvent by rotary evaporation and recrystallized from ethanol and acetone. The crystals were obtained by vacuum filtration to give 214mg (1.0 mmol; 28%) of 4,4'-azobis(pyridine-1-oxide).

^{1}H NMR (D_2O; 400Mhz): δ= 8.50 (d, J= 7.0 Hz, 2H); 8.09 (d, J= 7.0 Hz, 2H) ppm.

^{13}C NMR (D_2O; 100MHz): δ= 151.0 (C_4); 140.9 (C_2); 120.6 (C_3) ppm.

IR (CD_3CN): υ= 1605, 1470, 1275, 1144 cm^{-1}.

IR (Nujol mull): Identical to previously published data.[69]

UV-Vis (cyclohexane): λ_{max}= 440 nm. Solubility in hydrocarbon solvents is too low for reliable calculation of extinction coefficients.

MS (Electrospray): $C_{10}H_8N_4O_2Na$ (M+Na) required= 239.0545; actual= 239.0554

3.3.5- Kinetic Studies of 1,3-Dipolar Cycloaddition Reactions by HPLC

A typical experiment is as follows: 9.5mg of 4-azidopyridine-1-oxide, 25μL of methyl benzoate, and 1000μL of acetonitrile were combined in a 3mL reaction vial. To this solution were added 1500μL of methyl acrylate. The vial was then sealed and degassed with a thin stream of argon. A 50μL aliquot was withdrawn at time zero, and the vial placed in a 50° C oil bath. Subsequent 50μL aliquots were withdrawn at 30-minute intervals. All aliquots were placed into HPLC vials, diluted with 1000μL of 1:1 HPLC-grade methanol: Millipore water, and stored in a freezer until used for HPLC analysis. A complete set of reaction conditions can be found in Appendix A.

Table 1- HPLC Gradient Details

	Time (min)	Flow (mL/min)	%A	%B	%C	Curve
1	0.01	0.5	70	0	30	6
2	3	0.5	50	0	50	6
3	9	0.5	0	0	100	6
4	13	0.5	0	50	50	6
5	17	0.5	0	80	20	6
6	20	0.5	0	80	20	6
7	22	0.5	0	0	100	3
8	26	0.5	80	0	20	3
9	30	0.5	80	0	20	6

Solvent A: 100% Water; Solvent B: 100% Methanol; Solvent C: 1:1 Methanol:Water
Curve Details: 6= Linear; 3= Growing Exponential

Appendix A- Table of Conditions for Kinetic Experiments

Run #	1	2	3	4	5	6	7	8	9
Temp (°C)	50	50	50	50	50	50	50	50	50
4-azidopyridine-1-oxide (mg)	10.1	9.5	5.3	21.3	30.8	40.1	50.0	10.0	9.6
methyl benzoate (□L)	25	25	25	25	25	25	25	25	25
methyl acrylate (□L)	0	1500	1500	1500	1500	1500	1500	1200	1000
acetonitrile (□L)	2500	1000	1000	1000	1000	1000	1000	1300	1500
aliquot (□L)	50	50	50	50	40	30	20	50	50
50:50 H_2O/MeOH (□L)	1000	1000	1000	1000	1000	1000	1000	1000	1000
v. HPLC injection (□L)	5	5	10	5	5	5	5	5	5

Run #	10	11	12	13	14	15	16	17	18
Temp (°C)	50	50	50	50	50	50	50	50	50
4-azidopyridine-1-oxide (mg)	9.8	10.2	10.2	10.6	9.8	10.3	9.8	10.5	10.1
methyl benzoate (□L)	25	25	25	25	25	25	25	25	25
methyl acrylate (□L)	800	500	300	200	100	80	50	20	10
acetonitrile (□L)	1700	2000	2200	2300	2400	2450	2450	2500	2500
aliquot (□L)	50	50	50	50	50	50	50	50	50
50:50 H_2O/MeOH (□L)	1000	1000	1000	1000	1000	1000	1000	1000	1000
HPLC injection (□L)	5	5	5	5	5	5	5	5	5

Acetonitrile, methanol, water all HPLC grade
Methyl acrylate distilled before use.
All samples stored in freezer prior to HPLC analysis.

Appendix B- Kinetic Data: 1.3-Dipolar Cycloaddition Reaction

Table 2- Summary of Kinetic Data

Run #	[4-AP-1-O]	[Methyl Acrylate]	[Methyl Benzoate]	k_{obs} (s^{-1})	k_{cyc} ($M^{-1}s^{-1}$)
1	2.94E-02	0	7.9E-02	0	0
2	2.8E-02	6.520E+00	7.9E-02	7.13E-05	1.09E-05
3	1.5E-02	6.520E+00	7.9E-02	7.35E-05	1.13E-05
4	6.20E-02	6.520E+00	7.9E-02	8.03E-05	1.23E-05
5	8.96E-02	6.520E+00	7.9E-02	7.12E-05	1.09E-05
6	1.17E-01	6.520E+00	7.9E-02	7.25E-05	1.11E-05
7	1.45E-01	6.520E+00	7.9E-02	6.62E-05	1.01E-05
8	2.91E-02	5.216E+00	7.9E-02	4.80E-05	9.20E-06
9	2.8E-02	4.347E+00	7.9E-02	3.88E-05	8.93E-06
10	2.9E-02	3.48E+00	7.9E-02	3.08E-05	8.87E-06
11	2.97E-02	2.17E+00	7.9E-02	2.10E-05	9.66E-06
12	2.97E-02	1.30E+00	7.9E-02	1.35E-05	1.03E-05
13	3.08E-02	8.69E-01	7.9E-02	7.85E-06	9.03E-06
14	2.9E-02	4.35E-01	7.9E-02	3.08E-06	7.09E-06
15	2.96E-02	3.4E-01	7.8E-02	2.42E-06	7.03E-06
16	2.9E-02	2.2E-01	7.9E-02	2.00E-06	9.20E-06
17	3.03E-02	8.6E-02	7.8E-02	9.47E-07	1.10E-05
18	2.93E-02	4.3E-02	7.9E-02	4.98E-07	1.15E-05

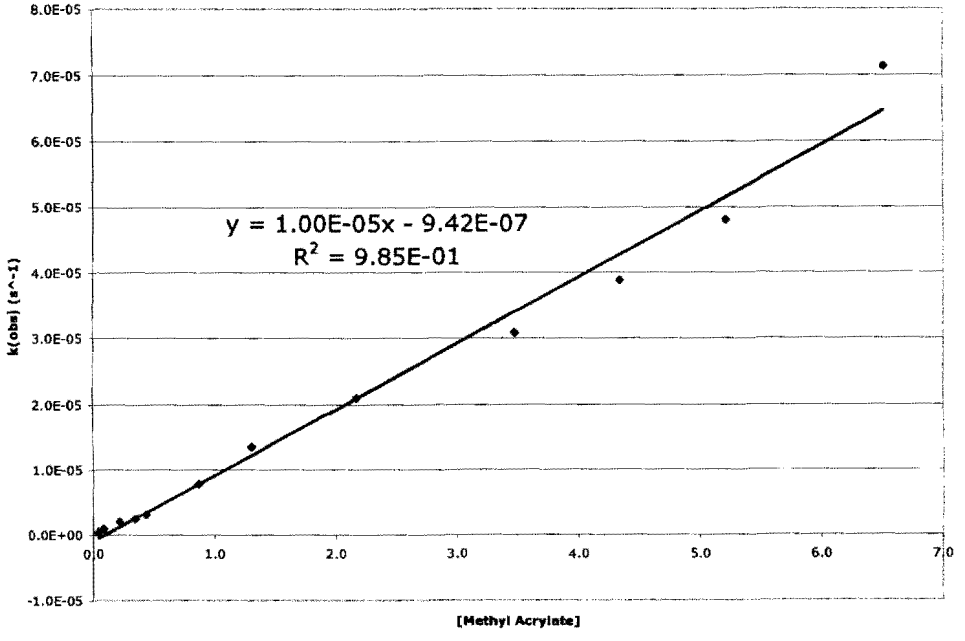

Table 3- Kinetic Run #2

Standardized Peak Area						First-Order Data
Time (s)	Unknown 1	4-AP-1-O	Unknown 2	Monoadduct	Diadduct	4-AP-1-O
0	0.0000	2.3885	0.0000	0.0000	0.0000	0.0000
900	0.0000	2.4908	0.0920	0.0000	0.2154	0.0419
1920	0.0377	2.1470	0.0523	0.0000	0.5121	-0.1066
2700	0.0575	2.0838	0.0000	0.0000	0.7255	-0.1365
3600	0.0783	2.0199	0.0334	0.0000	0.9651	-0.1676
4500	0.0949	1.8740	0.0297	0.0000	1.1406	-0.2426
5400	0.1155	1.7880	0.0000	0.0000	1.3317	-0.2896
6300	0.1402	1.6515	0.0000	0.0303	1.5032	-0.3690
7200	0.1650	1.4943	0.0000	0.0391	1.7051	-0.4690
8100	0.1892	1.3985	0.0000	0.0439	1.8389	-0.5353
9000	0.2194	1.3405	0.0000	0.0546	2.0284	-0.5776
9900	0.2389	1.2448	0.0000	0.0611	2.1355	-0.6517
10800	0.2634	1.1652	0.0000	0.0702	2.2399	-0.7178
11700	0.2914	1.1088	0.0000	0.0743	2.3581	-0.7674
12600	0.3203	1.0220	0.0000	0.0829	2.4766	-0.8489

1^{st}-Order Regression Analysis Parameters

			Amount	Conc. (M)
a	-7.13E-05			
b	6.03E-02	4-AP-1-O	9.5 mg	2.8E-02
R^2	0.985	Me. Acrylate	1500 uL	6.520E+00

Table 4- Kinetic Run #3

Standardized Peak Area						First-Order Data
Time (s)	Unknown 1	4-AP-1-O	Unknown 2	Monoadduct	Diadduct	4-AP-1-O
0	0.0000	1.3661	0.0000	0.0000	0.1090	0.0000
900	0.0208	1.3207	0.0178	0.0000	0.2290	-0.0338
1860	0.0501	1.2915	0.0163	0.0000	0.3844	-0.0562
2700	0.0699	1.1596	0.0143	0.0158	0.4641	-0.1639
3600	0.0887	1.0818	0.0000	0.0218	0.5644	-0.2334
4500	0.1084	1.0277	0.0000	0.0275	0.6702	-0.2846
5400	0.1263	0.9708	0.0000	0.0319	0.7622	-0.3417
6300	0.1380	0.8971	0.0000	0.0374	0.8432	-0.4205
7200	0.1658	0.8327	0.0000	0.0410	0.9422	-0.4951
8100	0.1759	0.7695	0.0000	0.0431	1.0259	-0.5740
9000	0.2012	0.7221	0.0000	0.0463	1.1294	-0.6375
9900	0.2061	0.6809	0.0000	0.0528	1.1849	-0.6964
10800	0.2187	0.6326	0.0000	0.0520	1.2088	-0.7699
11700	0.2294	0.6101	0.0000	0.0589	1.2720	-0.8061

1^{st}-Order Regression Analysis Parameters

			Amount	Conc. (M)
a	-7.35E-05			
b	6.33E-02	4-AP-1-O	5.3 mg	1.5E-02
R^2	0.995	Me. Acrylate	1500 uL	6.520E+00

Table 5- Kinetic Run #4

Standardized Peak Area						First-Order Data
Time (s)	Unknown 1	4-AP-1-O	Unknown 2	Monoadduct	Diadduct	4-AP-1-O
0	0.0000	5.7186	0.0000	0.0000	0.7891	0.0000
1800	0.1740	5.3085	0.0000	0.0783	1.7554	-0.0744
3600	0.3417	4.9628	0.0000	0.1325	2.8316	-0.1417
5400	0.4691	4.3503	0.0000	0.1763	3.6848	-0.2735
7200	0.5829	3.7919	0.0000	0.2148	4.3329	-0.4108
9000	0.6898	3.2014	0.0000	0.2472	5.0298	-0.5801
10800	0.8858	2.9004	0.0000	0.3074	6.1817	-0.6789
12600	0.9629	2.4112	0.0000	0.3291	6.6308	-0.8636
15720	1.3597	1.9980	0.0000	0.3934	8.7179	-1.0516
18000	1.3229	1.4594	0.0000	0.3911	8.3372	-1.3657
19800	1.3280	1.2625	0.0000	0.4377	4.1703	-1.5106
21600	1.2629	1.0246	0.0000	0.3573	2.3613	-1.7194
23400	1.4138	0.9953	0.0000	0.3789	2.0158	-1.7484

1st-Order Regression Analysis Parameters

			Amount	Conc. (M)
a	-8.03E-05			
b	1.19E-01	4-AP-1-O	21.4 mg	6.20E-02
R^2	0.989	Me. Acrylate	1500 uL	6.520E+00

Table 6- Kinetic Run #5

Standardized Peak Area						First-Order Data
Time (s)	Unknown 1	4-AP-1-O	Unknown 2	Monoadduct	Diadduct	4-AP-1-O
0	0.0648	8.9271	0.0379	0.0523	1.4667	0.0000
1800	0.2217	6.7538	0.0000	0.1053	2.4019	-0.2790
3600	0.4723	7.5530	0.0000	0.1822	3.7062	-0.1671
5400	0.6972	6.0117	0.0000	0.2720	5.4981	-0.3954
7200	0.9374	5.5283	0.0000	0.3490	6.9907	-0.4792
9000	1.0663	4.5537	0.0000	0.3791	7.6056	-0.6732
12000	1.4633	3.9207	0.0000	0.4741	9.9455	-0.8228
14400	1.5891	2.9531	0.0871	0.4875	6.6518	-1.1062
16200	1.6518	2.6046	0.0000	0.5063	2.2136	-1.2318
18000	1.8028	2.3980	0.0000	0.5330	1.8219	-1.3145
19800	2.0311	2.2837	0.0000	0.5602	1.7026	-1.3633

1st-Order Regression Analysis Parameters

			Amount	Conc. (M)
a	-7.11E-05			
b	1.74E-02	4-AP-1-O	30.8 mg	8.96E-02
R^2	0.980	Me. Acrylate	1500 uL	6.52E+00

Table 7- Kinetic Run #6

Standardized Peak Area						First-Order Data
Time (s)	Unknown 1	4-AP-1-O	Unknown 2	Monoadduct	Diadduct	4-AP-1-O
0	0.0846	12.7504	0.0000	0.0647	1.7832	0.0000
1800	0.3688	12.2775	0.0000	0.1779	3.6207	-0.0378
3600	0.7310	10.5001	0.0000	0.2998	6.0667	-0.1942
5400	1.0179	8.4674	0.0000	0.3811	7.8103	-0.4093
7200	1.4364	8.0893	0.0000	0.4843	10.2563	-0.4550
8160	1.7397	8.3063	0.0000	0.5810	12.4420	-0.4285
11580	2.0281	5.3394	0.0000	0.6013	13.1173	-0.8704
14400	2.1730	4.3662	0.0000	0.6649	2.7065	-1.0717
16200	2.4997	4.2242	0.0000	0.7379	2.3638	-1.1047
18000	2.8132	3.7697	0.0000	0.8077	2.4068	-1.2186

1st-Order Regression Analysis Parameters

a	-7.25E-05		Amount	Conc. (M)
b	4.69E-02	4-AP-1-O	40.1 mg	1.17E-01
R^2	0.980	Me. Acrylate	1500 uL	6.52E+00

Table 8- Kinetic Run #7

Standardized Peak Area						First-Order Data
Time (s)	Unknown 1	4-AP-1-O	Unknown 2	Monoadduct	Diadduct	4-AP-1-O
0	0.0000	13.0337	0.0000	0.0000	0.0000	0.0000
900	0.0000	12.3627	0.2257	0.0000	1.6093	-0.0529
1800	0.0000	11.4580	0.3948	0.0000	2.7364	-0.1288
2700	0.1267	11.2197	0.4883	0.0000	3.9271	-0.1499
3600	0.1615	9.9362	0.5322	0.0703	4.6015	-0.2714
4500	0.2663	9.4988	0.5444	0.1013	5.5482	-0.3164
5400	0.3150	8.9120	0.5961	0.1078	6.2714	-0.3801
6360	0.4627	8.5102	0.6017	0.1446	7.1141	-0.4263
7380	0.5538	7.7686	0.5876	0.1672	6.7265	-0.5174
8100	0.6215	7.5528	0.6073	0.1926	5.8458	-0.5456
9000	0.7426	7.0897	0.4055	0.2209	4.2516	-0.6089
10080	0.8931	6.5645	0.4748	0.2320	2.8586	-0.6859
11100	0.9814	6.2487	0.4581	0.2866	2.4526	-0.7352
11700	1.1009	5.9176	0.4063	0.2804	2.2384	-0.7896
12600	1.2158	5.6186	0.3832	0.3183	2.1372	-0.8415
13500	1.3460	5.2524	0.3316	0.3411	2.0354	-0.9089
14400	1.5547	5.0710	0.2926	0.3507	1.9678	-0.9440
15300	1.6091	4.7774	0.2688	0.4100	1.7034	-1.0036

1st-Order Regression Analysis Parameters

a	-6.62E-05		Amount	Conc. (M)
b	-8.14E-03	4-AP-1-O	50.0 mg	1.45E-01
R^2	0.998	Me. Acrylate	1500 uL	6.52E+00

Table 9- Kinetic Run #8

Standardized Peak Area						First-Order Data
Time (s)	Unknown 1	4-AP-1-O	Unknown 2	Monoadduct	Diadduct	4-AP-1-O
0	0.0000	2.7627	0.0000	0.0000	0.1540	0.0000
900	0.0281	2.7076	0.0272	0.0000	0.4158	-0.0201
1800	0.0588	2.6285	0.0319	0.0000	0.6106	-0.0498
2700	0.0846	2.5276	0.0366	0.0284	0.7614	-0.0889
3600	0.1006	2.3808	0.0409	0.0375	0.9190	-0.1488
4500	0.1281	2.3167	0.0365	0.0463	1.0885	-0.1761
5400	0.1356	2.0920	0.0390	0.0478	1.1713	-0.2781
6360	0.1540	2.0067	0.0433	0.0558	1.3349	-0.3197
7380	0.1805	1.9263	0.0384	0.0678	1.5188	-0.3606
8100	0.2118	1.8837	0.0353	0.0663	1.6157	-0.3830
9000	0.2193	1.7495	0.0318	0.0771	1.7107	-0.4569
10200	0.2450	1.6766	0.0329	0.0827	1.8431	-0.4995
10800	0.2511	1.5975	0.0324	0.0888	1.8948	-0.5478
11700	0.2831	1.5719	0.0285	0.0922	2.0562	-0.5639
12600	0.3124	1.4850	0.0000	0.0891	2.1219	-0.6208
13500	0.3324	1.4850	0.0000	0.1031	2.2019	-0.6208
14400	0.3546	1.4038	0.0000	0.1031	1.9847	-0.6770
15300	0.3545	1.3080	0.0000	0.1102	1.7462	-0.7477
16200	0.3843	1.2763	0.0660	0.1181	1.6185	-0.7723
17040	0.4434	1.2946	0.0000	0.1173	1.5243	-0.7580
18000	0.4591	1.2204	0.0485	0.1244	1.3869	-0.8171

1st-Order Regression Analysis Parameters				
a	-4.80E-05		Amount	Conc. (M)
b	8.68E-03	4-AP-1-O	10.0 mg	2.91E-02
R^2	0.991	Me. Acrylate	1200 uL	5.22E+00

Table 10- Kinetic Run #9

Standardized Peak Area						First-Order Data
Time (s)	Unknown 1	4-AP-1-O	Unknown 2	Monoadduct	Diadduct	4-AP-1-O
0	0.0000	2.3119	0.0000	0.0000	0.2305	0.0000
1800	0.0616	2.0409	0.0000	0.0000	0.5073	-0.1247
3600	0.1134	1.9997	0.0000	0.0383	0.8151	-0.1451
5400	0.1450	1.8771	0.0000	0.0526	1.0357	-0.2084
7380	0.1781	1.8162	0.0000	0.0628	1.2523	-0.2414
9000	0.2039	1.6367	0.0000	0.0633	1.3713	-0.3454
10800	0.2117	1.4510	0.0000	0.0756	1.5145	-0.4658
12600	0.2553	1.4002	0.0000	0.0790	1.7187	-0.5015
14400	0.2949	1.3588	0.0000	0.0838	1.7808	-0.5315
16200	0.3077	1.1818	0.0000	0.0897	1.6326	-0.6711
18000	0.3625	1.1598	0.0000	0.1032	1.5707	-0.6898
19800	0.4134	1.1490	0.0000	0.1005	1.3998	-0.6992
21600	0.3619	0.9474	0.0000	0.1135	1.1559	-0.8921
23520	0.4097	0.9483	0.0000	0.1199	1.1040	-0.8912
25200	0.3973	0.8270	0.0000	0.1201	0.9656	-1.0280

1st-Order Regression Analysis Parameters

a	-3.88E-05		Amount	Conc. (M)
b	-6.35E-03	4-AP-1-O	9.6 mg	2.80E-02
R^2	0.985	Me. Acrylate	1000 uL	4.35E+00

Table 11- Kinetic Run #10

Standardized Peak Area						First-Order Data
Time (s)	Unknown 1	4-AP-1-O	Unknown 2	Monoadduct	Diadduct	4-AP-1-O
0	0.0000	3.7151	0.0000	0.0000	0.0000	0.0000
1800	0.0000	3.4734	0.0584	0.0000	0.4944	-0.0673
3960	0.0000	3.3441	0.0718	0.0000	0.9213	-0.1052
5400	0.0388	3.1512	0.0869	0.0000	1.1364	-0.1646
7200	0.0558	3.0253	0.1031	0.0000	1.4073	-0.2054
9000	0.0881	3.0230	0.1230	0.0367	1.7520	-0.2062
10800	0.0964	2.7574	0.1700	0.0414	1.9299	-0.2981
14400	0.1401	2.4572	0.1514	0.0574	2.4356	-0.4134
16320	0.1686	2.3334	0.1869	0.0669	2.6410	-0.4651
18000	0.2034	2.2284	0.1866	0.0722	2.8357	-0.5111
19920	0.2380	2.0975	0.1806	0.0891	3.0662	-0.5716
21600	0.3348	2.3746	0.1972	0.1193	3.8847	-0.4476
23400	0.3353	1.7936	0.1972	0.1073	3.3517	-0.7282
25200	0.3537	1.6615	0.1552	0.1142	3.3781	-0.8047
27000	0.3947	1.6148	0.0972	0.1281	3.6092	-0.8332
86460	0.4259	0.2623	0.2680	0.1727	1.0457	-2.6506
88680	0.4416	0.2449	0.2519	0.1835	0.9994	-2.7192

1^{st}-Order Regression Analysis Parameters

a	-3.09E-05		Amount	Conc. (M)
b	3.08E-02	4-AP-1-O	9.8 mg	2.90E-02
R^2	0.995	Me. Acrylate	800 uL	3.48E+00

Table 12- Kinetic Run #11

Standardized Peak Area						First-Order Data
Time (s)	Unknown 1	4-AP-1-O	Unknown 2	Monoadduct	Diadduct	4-AP-1-O
0	0.0000	2.6589	0.0000	0.0000	0.0843	0.0000
1800	0.0000	2.6413	0.0000	0.0000	0.2940	-0.0066
3840	0.0354	2.5866	0.0000	0.0000	0.4857	-0.0276
5400	0.0500	2.4172	0.0000	0.0258	0.5827	-0.0953
7200	0.0643	2.3253	0.0356	0.0314	0.7099	-0.1341
9000	0.0787	2.2756	0.0264	0.0392	0.8485	-0.1556
10800	0.0960	2.1808	0.0270	0.0425	0.9608	-0.1982
14400	0.1317	2.0842	0.0286	0.0538	1.2170	-0.2435
16200	0.1508	1.9978	0.0277	0.0583	1.3321	-0.2858
18000	0.1685	1.9566	0.0274	0.0661	1.4629	-0.3067
19860	0.1863	1.8832	0.0270	0.0744	1.5876	-0.3450
21600	0.2059	1.7888	0.0297	0.0754	1.6546	-0.3964
23400	0.2239	1.7279	0.0000	0.0832	1.7790	-0.4310
25200	0.2525	1.7105	0.0000	0.0878	1.9055	-0.4411
27000	0.2709	1.6444	0.0000	0.0906	2.0140	-0.4805
86400	0.3880	0.4447	0.0648	0.1599	3.5722	-1.7883
88620	0.3972	0.4275	0.0620	0.1667	3.5989	-1.8277

1^{st}-Order Regression Analysis Parameters

a	-2.10E-05		Amount	Conc. (M)
b	4.57E-02	4-AP-1-O	10.2 mg	2.97E-02
R^2	0.998	Me. Acrylate	500 uL	2.17E+00

Table 13- Kinetic Run #12

Standardized Peak Area						First-Order Data
Time (s)	Unknown 1	4-AP-1-O	Unknown 2	Monoadduct	Diadduct	4-AP-1-O
0	0.0000	2.6162	0.0000	0.0000	0.0000	0.0000
3600	0.0000	2.7113	0.0424	0.0000	0.2735	0.0357
7200	0.0000	2.5972	0.0441	0.0000	0.5076	-0.0073
12840	0.0413	2.4402	0.0729	0.0000	0.8351	-0.0696
14400	0.0476	2.2370	0.0709	0.0000	0.8597	-0.1566
18000	0.0648	2.1753	0.0806	0.0000	1.0658	-0.1845
21600	0.0865	2.0361	0.1029	0.0252	1.2121	-0.2507
25200	0.1159	2.0334	0.1066	0.0315	1.4358	-0.2520
55380	0.1279	1.3459	0.1660	0.0457	2.5389	-0.6646
57600	0.1369	1.3023	0.1699	0.0493	2.5699	-0.6976
61200	0.1639	1.2440	0.1569	0.0546	2.6528	-0.7434
64980	0.1866	1.1955	0.1521	0.0672	2.7712	-0.7832
68400	0.2070	1.1335	0.1458	0.0700	2.6545	-0.8364
75780	0.2580	1.0524	0.1311	0.0839	2.1094	-0.9107
79200	0.2779	0.9740	0.1070	0.0902	1.8409	-0.9881
82800	0.3098	0.9483	0.0968	0.0958	1.7247	-1.0148
140760	0.5619	0.4139	0.0263	0.1283	1.2422	-1.8438
144000	0.5892	0.3920	0.0000	0.1310	1.2380	-1.8981
147600	0.6187	0.3826	0.0000	0.1310	1.2403	-1.9226

1st-Order Regression Analysis Parameters

a	-1.34E-05		Amount	Conc. (M)
b	7.07E-02	4-AP-1-O	10.2 mg	2.97E-02
R^2	0.998	Me. Acrylate	300 uL	1.30E+00

Table 14- Kinetic Run #13

Standardized Peak Area						First-Order Data
Time (s)	Unknown 1	4-AP-1-O	Unknown 2	Monoadduct	Diadduct	4-AP-1-O
0	0.0000	2.6382	0.0000	0.0000	0.0000	0.0000
3600	0.0000	2.7779	0.0000	0.0000	0.0000	0.0516
7200	0.0000	2.5582	0.0549	0.0000	0.2588	-0.0308
10800	0.0000	2.5480	0.0345	0.0000	0.4209	-0.0348
14400	0.0000	2.5071	0.0352	0.0000	0.5178	-0.0510
19020	0.0000	2.4054	0.0421	0.0000	0.5986	-0.0924
21720	0.0000	2.3701	0.0408	0.0000	0.6657	-0.1072
77340	0.1194	1.4921	0.1142	0.0535	1.9189	-0.5699

1st-Order Regression Analysis Parameters

a	-7.85E-06		Amount	Conc. (M)
b	4.68E-02	4-AP-1-O	10.6 mg	3.08E-02
R^2	0.983	Me. Acrylate	200 uL	8.69E-01

Table 15- Kinetic Run #14

Standardized Peak Area						First-Order Data
Time (s)	Unknown 1	4-AP-1-O	Unknown 2	Monoadduct	Diadduct	4-AP-1-O
0	0.0000	2.5143	0.0000	0.0000	0.0000	0.0000
7200	0.0000	2.4852	0.0000	0.0000	0.1334	-0.0116
14400	0.0000	2.5669	0.0000	0.0000	0.2476	0.0207
21600	0.0000	2.5048	0.0000	0.0000	0.3494	-0.0038
76920	0.0000	2.0479	0.0580	0.0000	0.9988	-0.2052
82800	0.0000	1.9749	0.0582	0.0304	1.0846	-0.2415
90000	0.0000	1.9760	0.0561	0.0351	1.1925	-0.2409

1st-Order Regression Analysis Parameters

a	-3.08E-06		Amount	Conc. (M)
b	3.14E-02	4-AP-1-O	9.8 mg	2.90E-02
R^2	0.958	Me. Acrylate	100 uL	4.35E-01

Table 16- Kinetic Run #15

Standardized Peak Area						First-Order Data
Time (s)	Unknown 1	4-AP-1-O	Unknown 2	Monoadduct	Diadduct	4-AP-1-O
0	0.0000	2.6359	0.0000	0.0000	0.0000	0.0000
7200	0.0000	2.6182	0.0000	0.0000	0.0000	-0.0068
14400	0.0000	2.5155	0.0000	0.0000	0.1852	-0.0468
21600	0.0000	2.4494	0.0583	0.0000	0.1943	-0.0734
76560	0.0000	2.1348	0.0000	0.0000	0.7332	-0.2109
82800	0.0000	2.1423	0.0362	0.0000	0.8174	-0.2073
90000	0.0000	2.1551	0.0366	0.0288	0.8921	-0.2014

1st-Order Regression Analysis Parameters

a	-2.42E-06		Amount	Conc. (M)
b	-5.50E-03	4-AP-1-O	10.3 mg	2.96E-02
R^2	0.974	Me. Acrylate	80 uL	3.40E-01

Table 17- Kinetic Run #16

Standardized Peak Area						First-Order Data
Time (s)	Unknown 1	4-AP-1-O	Unknown 2	Monoadduct	Diadduct	4-AP-1-O
0	0.0000	2.6496	0.0000	0.0000	0.0000	0.0000
10800	0.0000	2.6194	0.0000	0.0000	0.1351	-0.0115
21600	0.0280	2.4736	0.0000	0.0000	0.2442	-0.0688
86400	0.0821	2.2155	0.0453	0.0000	0.7657	-0.1789
97200	0.1029	2.2442	0.0452	0.0000	0.8740	-0.1661
108000	0.1191	2.2133	0.0440	0.0284	0.9646	-0.1799
172800	0.1598	1.8619	0.0685	0.0284	1.3382	-0.3528
183600	0.1875	1.8368	0.0601	0.0300	1.4137	-0.3664
194400	0.2219	1.8301	0.0392	0.0380	1.4969	-0.3700
259200	0.2402	1.6430	0.0640	0.0423	1.8880	-0.4779
270000	0.2464	1.4644	0.0460	0.0412	1.7695	-0.5930
280800	0.3102	1.5013	0.0307	0.0465	1.9784	-0.5681
345600	0.3359	1.3434	0.0361	0.0533	2.2044	-0.6792
363600	0.3446	1.2699	0.0287	0.0611	2.2358	-0.7355
374400	0.3517	1.2583	0.0342	0.0586	2.2588	-0.7447
432000	0.3387	1.0990	0.0440	0.0638	2.3707	-0.8801
442800	0.3794	1.1150	0.0269	0.0765	2.4619	-0.8656
453600	0.4072	1.0834	0.0000	0.0759	2.4673	-0.8943

1^{st}-Order Regression Analysis Parameters

a	-2.00E-06		Amount	Conc. (M)
b	3.84E-03	4-AP-1-O	9.8 mg	2.90E-02
R^2	0.995	Me. Acrylate	50 uL	2.20E-01

Table 18- Kinetic Run #17

Standardized Peak Area						First-Order Data
Time (s)	Unknown 1	4-AP-1-O	Unknown 2	Monoadduct	Diadduct	4-AP-1-O
0	0.0000	2.9335	0.0000	0.0000	0.0000	0.0000
14400	0.0000	3.1498	0.0000	0.0000	0.0739	0.0711
28800	0.0000	2.7569	0.0000	0.0000	0.1306	-0.0621
86400	0.0308	2.6883	0.0270	0.0000	0.3618	-0.0873
100800	0.0394	2.5687	0.0321	0.0000	0.3933	-0.1328
115200	0.0567	2.8651	0.0295	0.0000	0.4875	-0.0236
172800	0.0717	2.6232	0.0463	0.0000	0.6584	-0.1118
187200	0.0803	2.5079	0.0323	0.0000	0.6863	-0.1567
201600	0.0964	2.3354	0.0000	0.0000	0.6711	-0.2280
259200	0.1054	2.2167	0.0321	0.0000	0.8158	-0.2802
273600	0.1258	2.3420	0.0299	0.0000	0.9078	-0.2252
288000	0.1385	2.2484	0.0000	0.0270	0.9093	-0.2660
345600	0.1471	2.0891	0.0275	0.0287	1.0172	-0.3395
363600	0.1719	2.1842	0.0000	0.0324	1.1079	-0.2950
374400	0.1749	2.1408	0.0000	0.0337	1.1133	-0.3150
432000	0.1750	1.9298	0.0000	0.0335	1.1585	-0.4188
446400	0.1884	1.9637	0.0000	0.0373	1.2206	-0.4014
468000	0.2035	1.9164	0.0000	0.0457	1.2755	-0.4258

1st-Order Regression Analysis Parameters

			Amount	Conc. (M)
a	-9.47E-07			
b	1.33E-02	4-AP-1-O	10.5 mg	3.03E-02
R^2	0.933	Me. Acrylate	20 uL	8.60E-02

Table 19- Kinetic Run #18

Standardized Peak Area						First-Order Data
Time (s)	Unknown 1	4-AP-1-O	Unknown 2	Monoadduct	Diadduct	4-AP-1-O
0	0.0000	3.3491	0.0000	0.0000	0.0000	0.0000
28800	0.0000	3.5817	0.0000	0.0000	0.0872	0.0671
86400	0.0366	3.4480	0.0000	0.0000	0.2593	0.0291
115200	0.0539	3.4233	0.0000	0.0000	0.3059	0.0219
172800	0.0659	3.0251	0.0000	0.0000	0.3815	-0.1017
201600	0.0860	3.1989	0.0000	0.0000	0.4477	-0.0459
259200	0.0920	2.9525	0.0000	0.0000	0.5405	-0.1260
288000	0.1114	3.1763	0.0000	0.0000	0.6150	-0.0530
345600	0.1165	2.8689	0.0000	0.0000	0.6519	-0.1548
374400	0.1270	2.8421	0.0000	0.0000	0.6938	-0.1641
432000	0.1356	2.7416	0.0000	0.0000	0.7704	-0.2001
468000	0.1592	2.9239	0.0000	0.0000	0.8520	-0.1358

1st-Order Regression Analysis Parameters

			Amount	Conc. (M)
a	-4.99E-07			
b	4.33E-02	4-AP-1-O	10.1 mg	2.93E-02
R^2	0.789	Me. Acrylate	20 uL	4.30E-02

Appendix C- NMR Spectral Data

Figure 16- ^{1}H NMR of 4-Chloropyridine-1-Oxide in $CDCl_3$

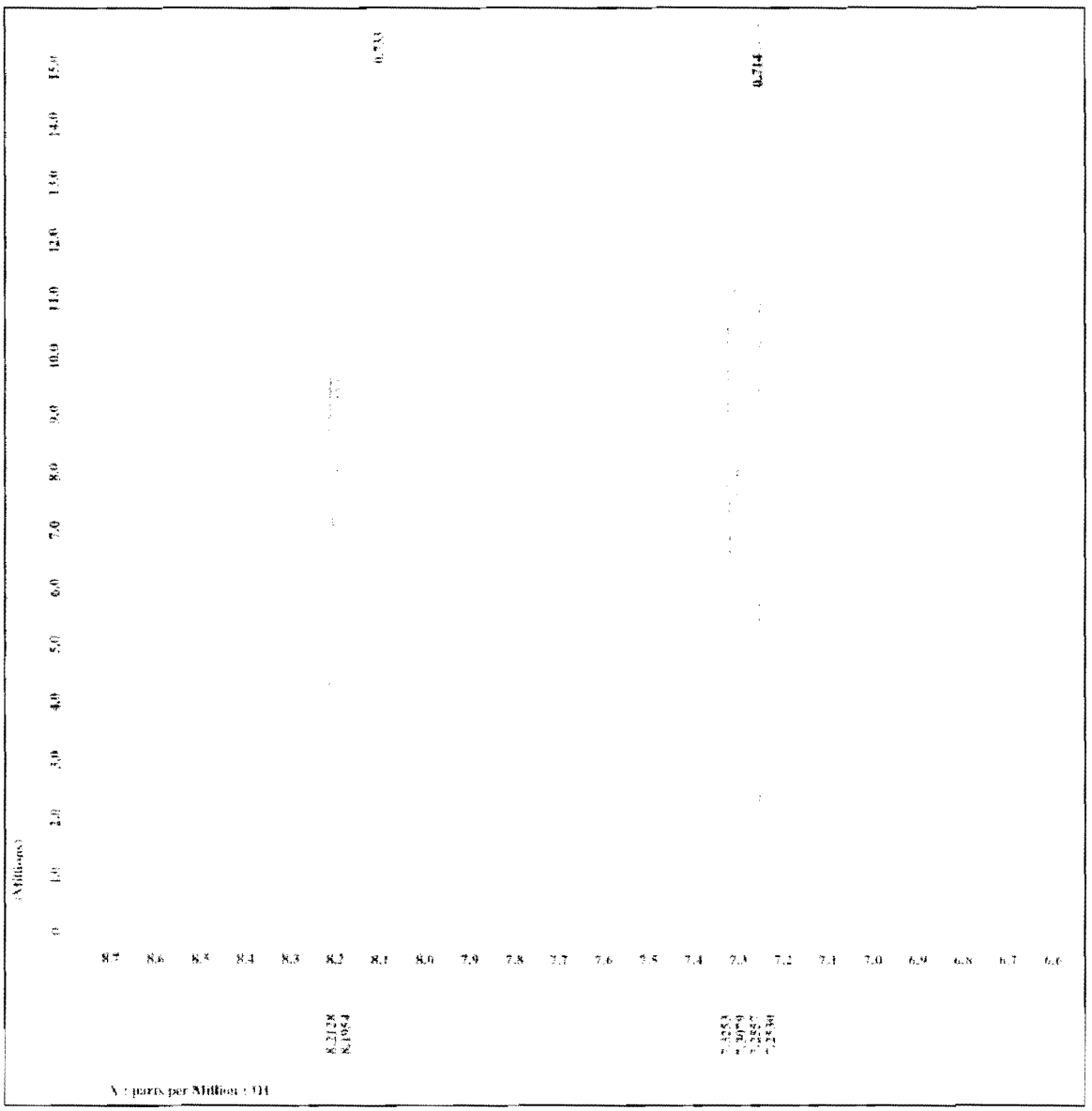

Figure 17- ^{1}H NMR of 4-Azidopyridine-1-Oxide in $CDCl_3$

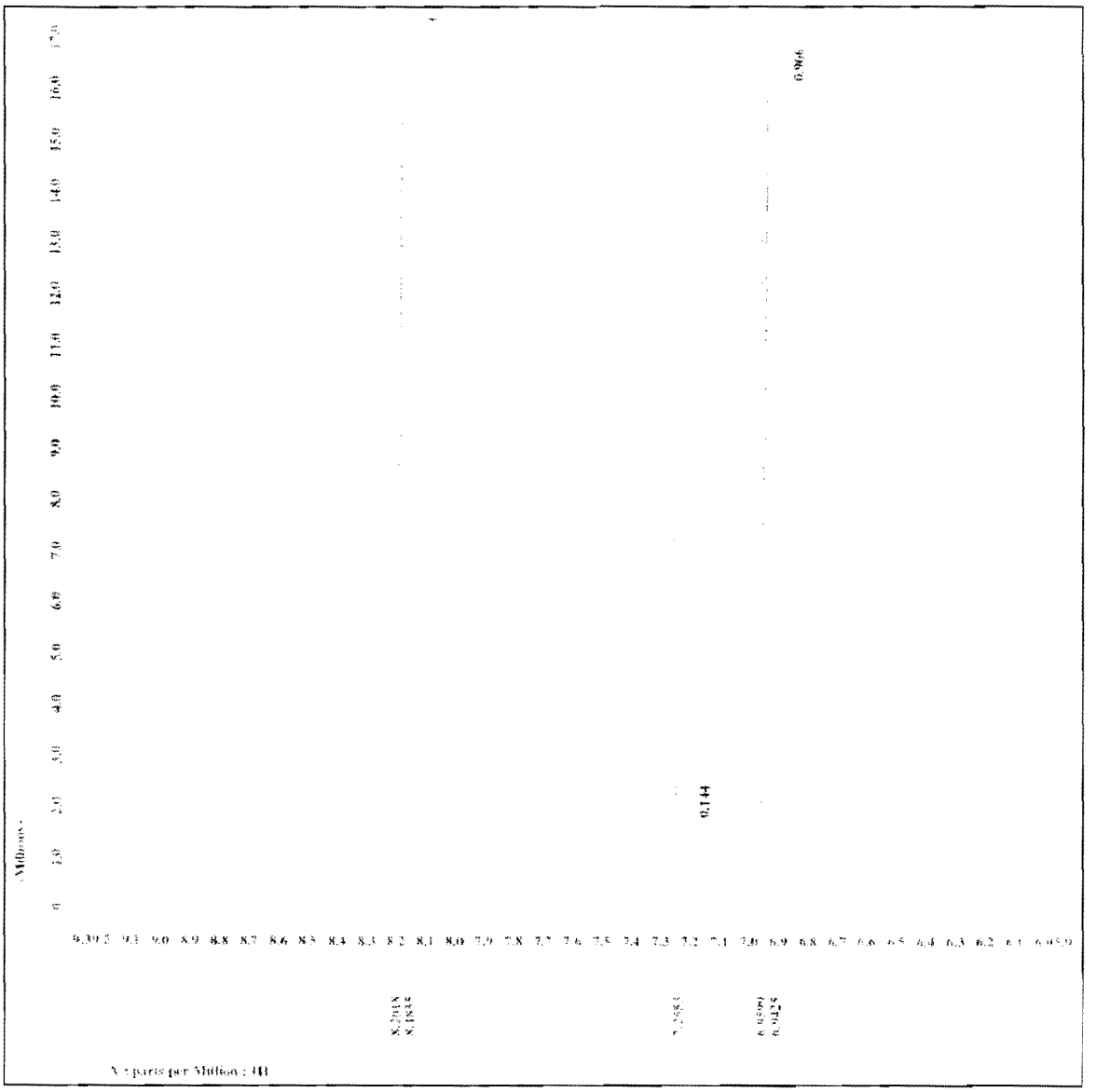

Figure 18- ^{13}C NMR of 4-Azidopyridine-1-Oxide in $CDCl_3$

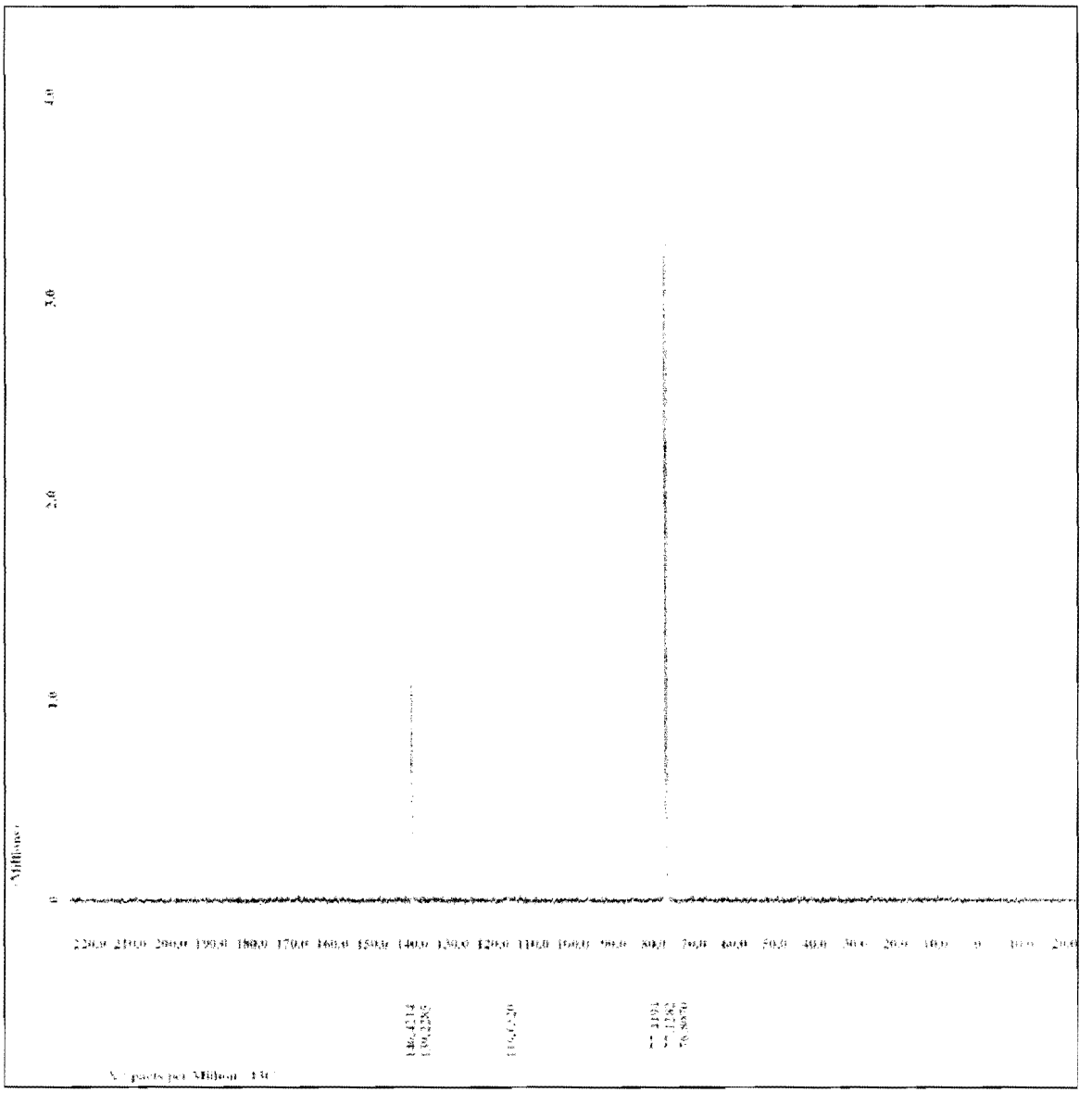

Figure 19- ^{1}H NMR of 4-Azidopyridine-1-Oxide in D_2O

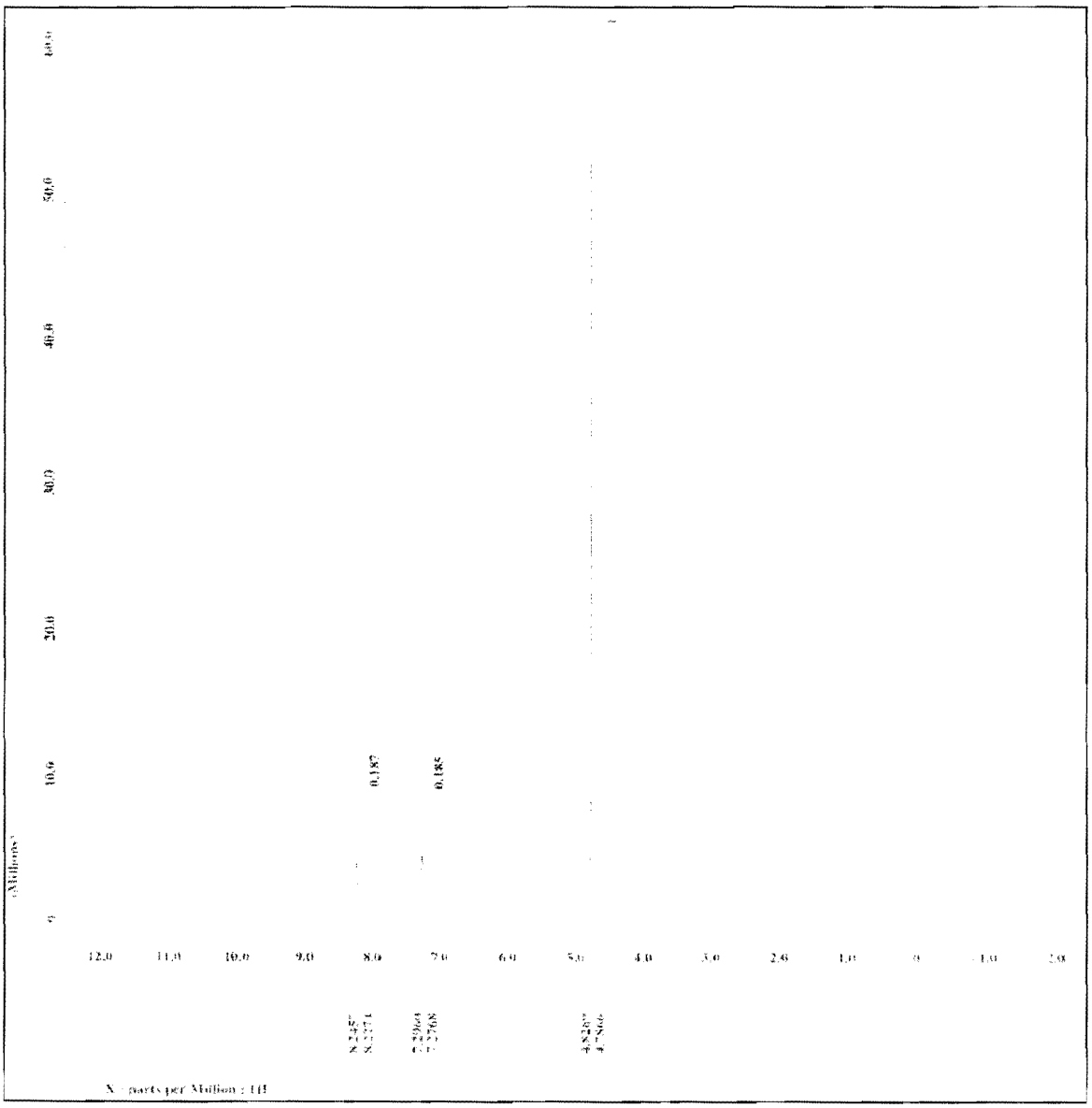

Figure 20- ^{1}H NMR of 4,4'-Azobis(Pyridine-1-Oxide) in D_2O

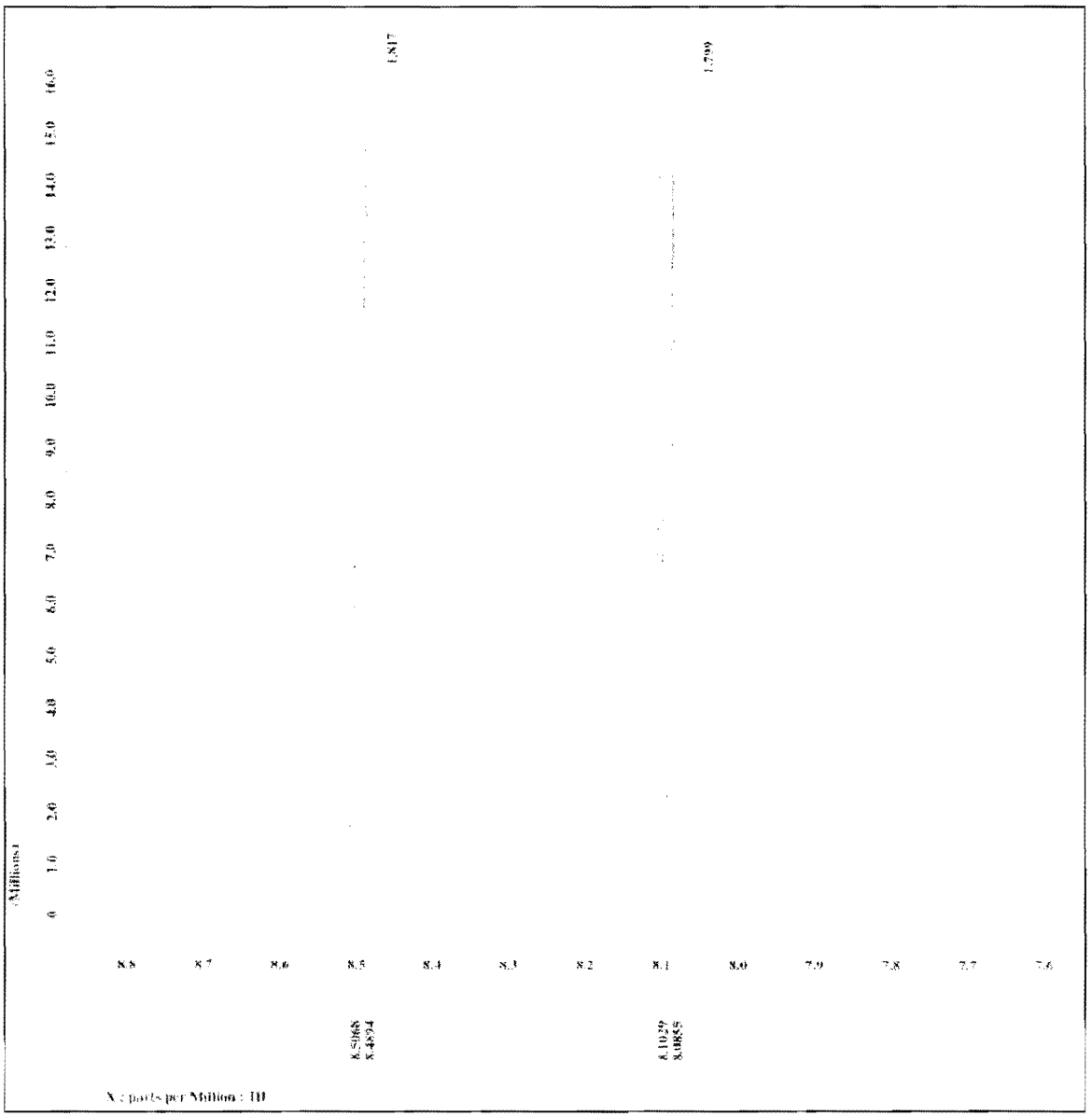

Figure 21- ^{13}C NMR of 4,4'-Azobis(Pyridine-1-Oxide) in D_2O

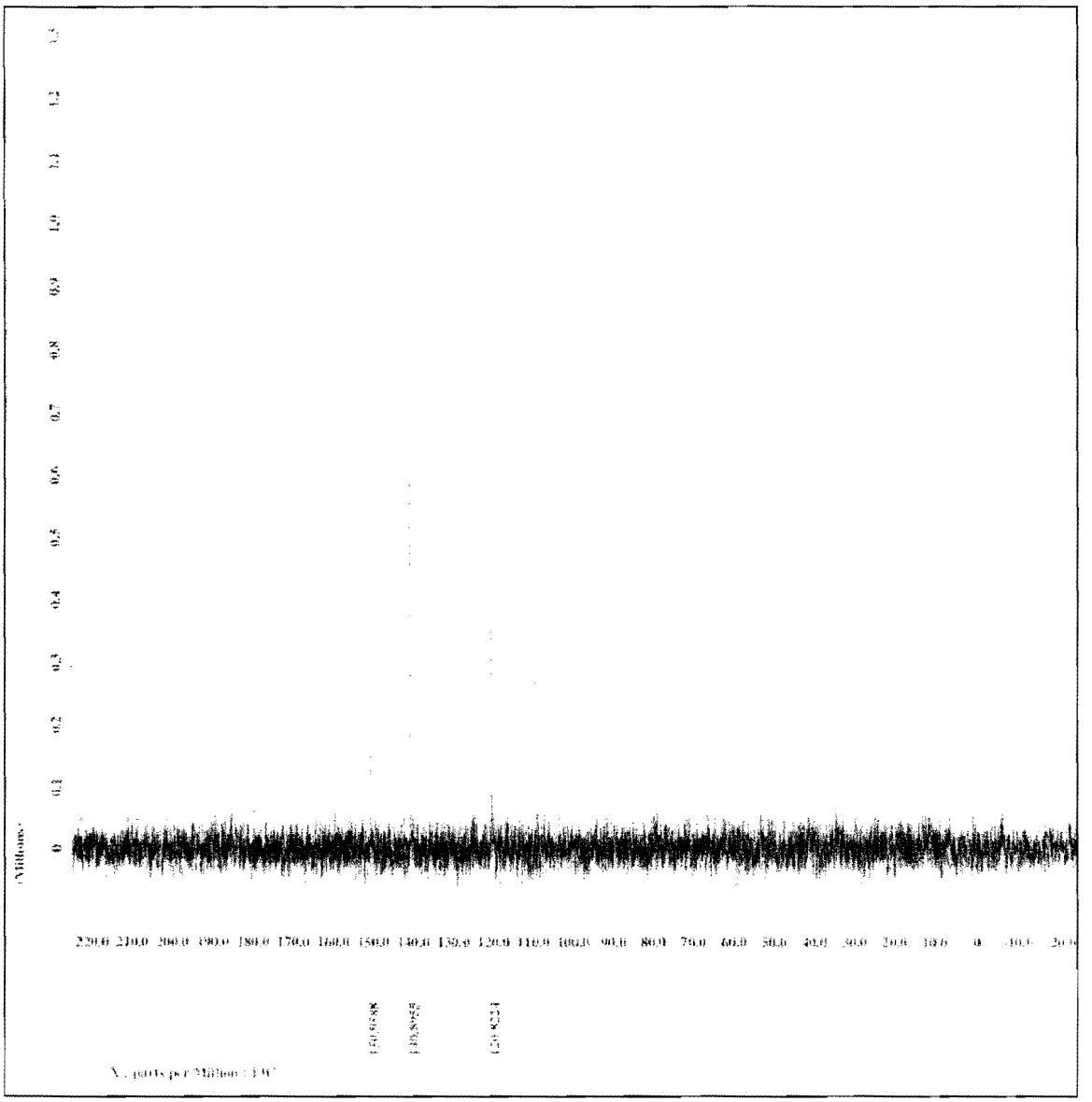

Figure 22- ^{1}H NMR of 3-Azidopyridine-1-Oxide in D_2O

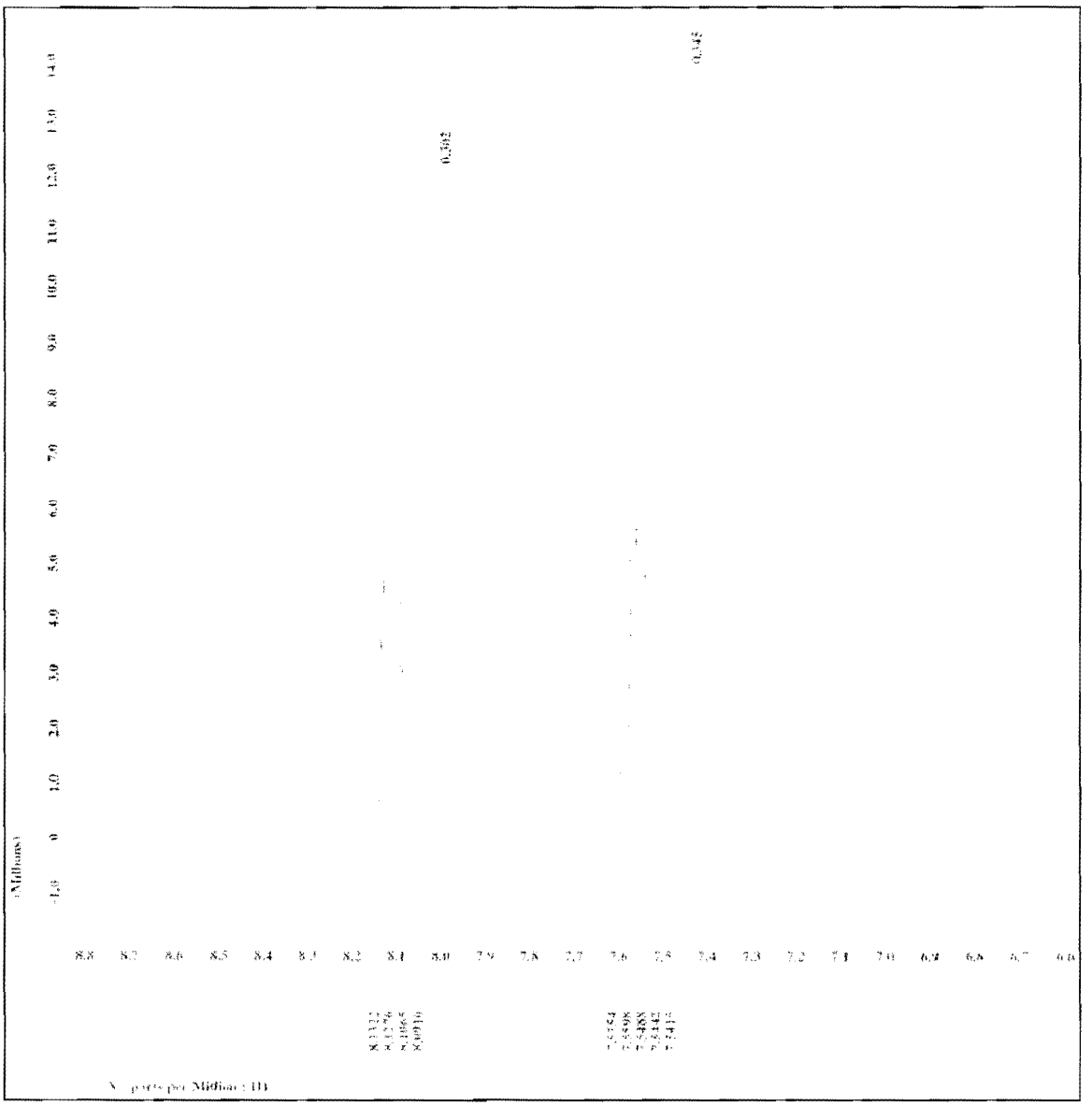

Appendix D- References

[1]Breslow, D. S. In *Azides and Nitrenes; Reactivity and Utility*; Scriven, E. F. V. Ed.; Academic Press: New York, 1984; 491.

[2]Trundle, C. U.S. Patent No. 4942113; 1990.

[3]Meijer, E. W.; Nijhuis, S.; Von Vroonhoven, F. C. B. M. *J. Am. Chem. Soc.* **1988**; *110*; 7209.

[4]Schnapp, K. A.; Platz, M. S. *Bioconjugate Chem.* **1993**; *4*; 178.

[5]Bayley, H. In *Photogenerated Reagents in Biochemistry and Molecular Biology;* Elsevier: New York, 1983.

[6]Smith, P. A. S. In *Nitrenes*; Lwowski, W. Ed.; Wiley-Interscience: New York, 1970; 99.

[7]Ternøe, C. W.; Christiansen, C.; Meldal, M.; *J. Org. Chem.* **2002**; *67*; 3057.

[8]Kadaba, P. K.; *J. Org. Chem.* **1992**; *57*; 3075.

[9]Dyall, L. K.; Smith, P. A. S. *Aust. J. Chem. Soc.* **1990**; *43*; 997.

[10]Marcinek, A.; Leyva, E.; Whitt, D.; Platz, M. S. *J. Am. Chem. Soc.* **1993**; *115*; 8609.

[11]Borden, W. T.; Gritsan, N. P.; Hadad, C. M.; Kerney, W. L.; Kemnitz, C. R.; Platz, M.S. *Acc. Chem. Res.* **2000**; *33*; 765.

[12]Admasu, A.; Gudmundsdóttir, A. D.; Platz, M. S. *J. Phys. Chem. A* **1997**; *101*; 3832.

[13](a) Kim, S. -J.; Hamilton, T. P.; Schaefer, H. F. *J. Am. Chem. Soc.* **1992**; *111*, 5349. (b) Hrovat, D. A.; Waali, E. E.; Borden, W. T. *J. Am. Chem. Soc.* **1992**; *114*; 8698-9.

[14]Borden, W. T. In *Diradicals*; Borden, W. T. Ed.; Wiley-Interscience: New York, 1982; 1-72.

[15]Drzaic, P. S.; Brauman, J. I. *J. Am. Chem. Soc.* **1984**; *106*; 3443.

[16]McDonald, R. N.; Davidson, S. J. *J. Am. Chem. Soc.* **1993**; *115*; 10857.

[17]Karney, W. L.; Borden, W. T. *J. Am. Chem. Soc.* **1997**; *119*; 1378.

[18]Schuster, G. B.; Platz, M. S. *Adv. Photochem.* **1992**; *17*; 69.

[19](a) Huigsen, R. *Angew Chem.* **1955**; *91*; 756. (b) Huigsen, R.; Vassius, D.; Appl, M. *Chem. Ber.* **1958**; *91*; 1. (c) Huigsen, R.; Appl, M. *Chem. Ber.* **1958**; *91*; 12.

[20]Doering, W. E.; Odum, R. A. *Tetrahedron* **1996**; *22*; 93.

[21]Schrock, A. K.; Schuster, G. B. *J. Am. Chem. Soc.* **1984**; *106*; 5228.

[22]Gritsan, N. P.; Zhai, H. B.; Yuzawa, T.; Karweik, D.; Brooke, J.; Platz, M. S. *J. Phys. Chem. A* **1997**; *101*; 2833.

[23]Leyva, E.; Platz, M. S.; Persy, G.; Wirz, J. *J. Am. Chem. Soc.* **1986**; *108*; 3783.

[24]Chapman, O. L.; Le Roux, J. –P. *J. Am. Chem. Soc.* **1978**; *100*; 282.

[25]Li, Y. Z.; Kirby, J. P.; George, M. W.; Poliakoff, M.; Schuster, G. *J. Am. Chem. Soc.* **1988**; *110*; 8092.

[26]Culllin, D. W.; Soundararajan, N.; Platz, M. S.; Miller, T. A. *J. Phys. Chem. A* **1990**; *94*; 5890.

[27]Carroll, S. E.; Nay, B.; Scriven, E. F. V.; Suschitzky, H.; Thomas, D. R. *Tetrahedron Lett.* **1977**; *18*; 3175.

[28]Gritsan, N. P.; Yuzawa, T.; Platz, M. S. *J. Am. Chem. Soc.* **1997**; *119*; 5059.

[29]Born, R.; Burda, C.; Senn, P.; Wirz, J. *J. Am. Chem. Soc.* **1997**; *119*; 5061.

[30]Tsao, M. –L; Platz, M. S. *J. Am. Chem. Soc.* **2003**; *125*; 12014.

[31]Gritsan, N. P.; Zhu, Z.; Hadad, C. M.; Platz, M. S. *J. Am. Chem. Soc.* **1999**; *121*; 1202.

[32]Gritsan, N. P.; Tigelaar, D.; Platz, M. S. *J. Phys. Chem. A* **1999**; *103*; 4465.

[33]Gritsan, N. P.; Likhotvorik, I.; Tsao, M. –L.; Çelebi, N.; Platz, M. S.; Karney, W. L.; Kennitz, C. R.; Borden, W. T. *J. Am. Chem. Soc.* **2001**; *123*; 1425.
[34]Tsao, M. –L.; Gritsan, N. P.; James, T. R.; Platz, M. S.; Hrovat, D.; Borden, W. T. *J. Am. Chem. Soc.* **2003**; *125*; 9343.
[35]Gritsan, N. P.; Platz, M. S. *Chem. Rev.* **2006**; *106*; 3844.
[36]Gritsan, N. P.; Gudmundsdóttir, A. D.; Tigelaar, D.; Platz, M. S. *J. Phys. Chem. A* **1999**; *103*; 3458.
[37]Gritsan, N. P.; Gudmundsdóttir, A. D.; Tigelaar, D.; Zhu, Z.; Karney, W. L.; Hadad, C.M.; Platz, M. S. *J. Am. Chem. Soc.* **2001**; *123*; 1951.
[38]Karney, W. L.; Borden, W. T. *J. Am. Chem. Soc.* **1997**; *119*; 3347.
[39](a) Smith, P. A. S.; Brown, B. B. *J. Am. Chem. Soc.* **1951**; *73*; 2438. (b) Smith, P. A. S.; Brown, B. B. *J. Am. Chem. Soc.* **1951**; *73*; 2435. (c) Smith, P. A. S.; Hall, J. H. *J. Am. Chem. Soc.* **1962**; *84*; 1632.
[40]Swenton, J.; Ikeler, T.; Williams, B. *J. Am. Chem. Soc.* **1970**; *72*; 3103.
[41]Speers, A. E.; Adam, G. C.; Cravatt, B. F. *J. Am. Chem. Soc.* **2003**; *125*; 4686.
[42]Wang, Q.; Chan, T. R.; Hilgraf, R.; Fokin, V. V.; Sharpless, B.; Finn, M. G. *J. Am. Chem. Soc.* **2003**; *125*; 3192.
[43]Lee, L. V.; Mitchell, M. L.; Huang, S. –J.; Fokin, V. V.; Sharpless, B.; Wong, C. –H. *J. Am. Chem. Soc.* **2003**; *125*; 9588.
[44]Lummerstorfer, T.; Hoffmann, H. *J. Phys. Chem. B* **2004**; *108*; 3963.
[45]Link, A. J.; Tirrell, D. A. *J. Am. Chem. Soc.* **2003**; *125*; 11164.
[46]Helms; B.; Mynar, J. L.; Hawker, C. J.; Fréchet, J. M. J. *J. Am. Chem. Soc.* **2004**; *126*; 15020.
[47]Wolff, L.; *Ann.* **1912**; *394*; 23.
[48]Huigsen, R. *Proc. Chem. Soc.* **1961**; 357.
[49]Scheiner, P.; Schomaker, J. H.; Deming, S.; Libbey, W. J. *J. Am. Chem. Soc.* **1965**; *87*; 306.
[50]Wijnen, J. W.; Steiner, R. A.; Engberts, J. B. F. N. *Tetrahedron Lett.* **1995**; *36*; 5389.
[51]Anderson, G. T.; Henry, J. R.; Weinreb, S. M. *J. Org. Chem.* **1991**; *56*; 6946.
[52]Huigsen, R.; Szeimies, G.; Möbius, L. *Chem. Ber.* **1966**; *99*; 475.
[53]Sustmann, R.; Trill, H. *Angew. Chem. Int. Ed. Engl.* **1972**; *11*; 838.
[54]L' Abbé, G. *Chem. Rev.* **1969**; *69*; 345.
[55]Crow, W. D.; Wentrup, C. *J. Chem. Soc. Chem. Commun.* **1968**; 1082.
[56]Wentrup, C.; Crow, W. D. *J. Chem. Soc. Chem. Commun.* **1969**; 1386.
[57]Sawanishi, H.; Tajima, K.; Tsuchiya, T. *Chem. Pharm. Bull.*; **1987**; *35*; 4101.
[58]Bednarek, P.; Wentrup, C. *J. Am. Chem. Soc.* **2003**; *125*; 9083.
[59]Kanyalkar, M.; Coutinho, E. C. *Tetrahedron* **2000**; *56*; 8775.
[60]Pietrzycki, W.; Tomasik, P. *Polish J. Chem.* **1998**; *72*; 893.
[61]Abramovitch, R. A.; Bachowska, B.; Tomasik, P. *Polish J. Chem.* **1984**; *58*; 805.
[62]Hostetler, K. J.; Crabtree, K. N.; Poole, J. S. *J. Org. Chem.* **2006**; *71*; 9023.
[63]Abramovitch, R. A.; Cue Jr., B. W. *J. Org. Chem.* **1973**; *38*; 173.
[64]Abramovitch, R. A.; Cue Jr., B. W. *J. Am. Chem. Soc.* **1976**; *98*; 1478.
[65]Hostetler, K. J. *M. S. Thesis*, Ball State University, 2005.
[66]Chapyshev, S.V., Kuhn, A; Wong, M.W.; Wentrup, C. *J. Am. Chem. Soc.* **2000**; *122*; 1572.
[67]Ochai, E. *J. Org. Chem.* **1953**; *18*; 534.

[68]Katritzky, A.R. *J. Am. Chem. Soc. Abstracts*; **1956**; 2404.
[69]Muniz-Miranda, M.; Pergolese, B.; Sbrana, G.; Bigotto, A. *J. Mol. Struct.*; **2005**; *744-747*; 339-43.